Applied Numerical Mathematics 151 (2020) 44–63

Contents lists available at ScienceDirect

Applied Numerical Mathematics

www.elsevier.com/locate/apnum

A spatial fourth-order maximum principle preserving operator splitting scheme for the multi-dimensional fractional Allen-Cahn equation

Dongdong He [a], Kejia Pan [b], Hongling Hu [c,*]

[a] School of Science and Engineering, The Chinese University of Hong Kong, Shenzhen, Guangdong 518172, China
[b] School of Mathematics and Statistics, Central South University, Changsha, Hunan 410083, China
[c] Key Laboratory of Computing and Stochastic Mathematics (Ministry of Education), School of Mathematics and Statistics, Hunan Normal University, Changsha, Hunan 410081, China

A R T I C L E   I N F O

Article history:
Received 25 August 2019
Received in revised form 5 November 2019
Accepted 19 December 2019
Available online 30 December 2019

Keywords:
Space fractional Allen-Cahn equation
Operator splitting method
Unconditional stability
Discrete maximum principle
ADI method

A B S T R A C T

In this paper, we consider the numerical study for the multi-dimensional fractional-in-space Allen-Cahn equation with homogeneous Dirichlet boundary condition. By utilizing Strang's second-order splitting method, at each time step, the numerical scheme can be split into three sub-steps. The first and third sub-steps give the same ordinary differential equation, where the solutions can be obtained explicitly. While a multi-dimensional linear fractional diffusion equation needs to be solved in the second sub-step, and this is computed by the Crank-Nicolson scheme together with alternating directional implicit (ADI) method. Thus, instead of solving a multidimensional nonlinear problem directly, only a series of one-dimensional linear problems need to be solved, which greatly reduces the computational cost. A fourth-order quasi-compact difference scheme is adopted for the discretization of the space Riesz fractional derivative of $\alpha (1 < \alpha \leq 2)$. The proposed method is shown to be unconditionally stable in L^2-norm, and satisfying the discrete maximum principle under some reasonable time step constraint. Finally, numerical experiments are given to verify our theoretical findings.

1. Introduction

The Allen-Cahn equation was first introduced by Allen and Cahn [1] to describe the motion of phase boundary in crystalline solids. The Allen-Cahn equation has been extensively studied and applied to many kinds of moving interface problems, for instance, cell membranes, the nucleation of solids and two-phase fluid flows [9–11,28,51,54,56]. Since the exact solution of the Allen-Cahn equation can not be found, numerical computations play an important role in the study of the Allen-Cahn equation. The Allen-Cahn equation has already been numerically investigated by many authors, see reference therein [7,12,13,19,23,24,38,39,43,49,50,58,60]. For example, the Allen-Cahn equation was numerically extensively studied by the operator splitting scheme [23,24,49]. It is well known that the Allen-Cahn equation has two intrinsic properties: free energy decay and the maximum principle [10]. Therefore, it is important to preserve these properties when designing the numerical schemes. For instance, an unconditionally stable nonlinear scheme with both discrete maximum principle and

* Corresponding author.
E-mail addresses: hedongdong@cuhk.edu.cn (D. He), kejiapan@csu.edu.cn (K. Pan), honglinghu@hunnu.edu.cn (H. Hu).

https://doi.org/10.1016/j.apnum.2019.12.018
0168-9274/

energy decay property was proposed by Choi et al. [7]. The discrete energy stability is examined in [12,13,19,39,60]. And the discrete maximum principle is investigated in [38,43]. However, the implicit-explicit scheme proposed in [43] is only first-order accurate in time, and it was pointed out that it still remains open to see whether the discrete maximum principle is true for high-order linear schemes [43].

In recent years, fractional differential equations have received many attention. For time-fractional diffusion equations, finite difference methods and spectral methods have been adopted [22,25,27,53,57]. For space fractional differential equations, there are also a lot of numerical studies for different type of equations [2,3,8,17,20,21,26,29,33–35,37,40,44–48,52,55, 59,61,62]. In particular, for the space fractional Allen-Cahn equation, Bueno-Orovio et al. [2] used an implicit finite element method, Burrage et al. [3] applied a Fourier spectral method, and Hou et al. [20] exploited a finite difference scheme. The space fractional Allen-Cahn equation also has the free energy decay property and the maximum principle. Although the method of [38,43] used for the integer order Allen-Cahn equation can be easily extended to the space fractional Allen-Cahn equation with the discrete maximum principle, these methods have only first-order accuracy in time. The recent scheme proposed by Hou et al. [20] for solving the space fractional Allen-Cahn equation is second-order accurate both in time and space. However, it is a nonlinear scheme and there is no dimensional splitting technique incorporated for the multi-dimensional problem. Therefore, the method of [20] will generally be computationally expensive especially when solving the three-dimensional (3D) problems. The ADI technique was utilized by Song et al. [40] to solve the two-dimensional (2D) space fractional Allen-Cahn equation together with the incompressible two-phase Navier-Stokes equations. An extra linear stabilized term is added into the system in order to obtain the unconditional stability. Similar treatments for the integer order Allen-Cahn equation can also be found in [38,43,58]. As far as we aware, there is no study on high-order maximum principle preserving schemes for the space fractional Allen-Cahn equation, which is considered as an open problem even in the case of the integer order Allen-Cahn equation [43].

In this paper, we consider the following multidimensional space fractional Allen-Cahn equation [2,3,5,14,20,30]

$$u_t = \varepsilon^2 L_\alpha u + u - u^3, \quad \mathbf{x} \in \Omega, \quad t \in (0, T], \tag{1.1}$$

with initial condition

$$u(\mathbf{x}, 0) = u_0(\mathbf{x}), \quad \mathbf{x} \in \Omega, \tag{1.2}$$

and the homogeneous Dirichlet boundary condition

$$u(\mathbf{x}, t) = 0, \quad \mathbf{x} \text{ on } \partial\Omega, \quad t \in [0, T], \tag{1.3}$$

where Ω is a rectangular 3D domain ($\Omega = [a, b]^3$) or 2D domain ($\Omega = [a, b]^2$), $\alpha \in (1, 2]$, ε is a positive number and L_α denotes the 3D Riesz fractional derivative operator (see the following paragraph). If $\alpha = 2$, then the above fractional Allen-Cahn equation reduces into the standard Allen-Cahn equation.

To define the operator L_α, we start from the definition in one dimension. The 1D Riesz fractional derivative $L_\alpha u$ ($\alpha \in (1, 2]$) for u defined in the interval $x \in [a, b]$ with homogeneous Dirichlet boundary condition is given as follows,

$$\mathcal{L}_\alpha u = \mathcal{L}_x^\alpha u := \frac{1}{-2\cos(\frac{\alpha\pi}{2})} \left({}_aD_x^\alpha u + {}_xD_b^\alpha u \right),$$

where ${}_aD_x^\alpha u$ and ${}_xD_b^\alpha u$ are the left and right Riemann-Liouville fractional derivatives, respectively given by

$${}_aD_x^\alpha u = \frac{1}{\Gamma(2-\alpha)} \frac{d^2}{dx^2} \int_a^x \frac{u(\xi)}{(x-\xi)^{\alpha-1}} d\xi, \quad {}_xD_b^\alpha u = \frac{1}{\Gamma(2-\alpha)} \frac{d^2}{dx^2} \int_x^b \frac{u(\xi)}{(\xi - x)^{\alpha-1}} d\xi.$$

The 3D Riesz fractional derivative $\mathcal{L}_\alpha u$ is defined as

$$\mathcal{L}_\alpha u = \mathcal{L}_x^\alpha u + \mathcal{L}_y^\alpha u + \mathcal{L}_z^\alpha u.$$

In addition, the fractional Allen-Cahn equation can be regarded as the L^2-gradient flow of the following fractional analogue Ginzburg-Landau free energy functional

$$\mathcal{E}(u) = \int_\Omega \left(\frac{1}{4}(u^2 - 1)^2 - \frac{1}{2}\varepsilon^2 u L_\alpha u \right) du. \tag{1.4}$$

In this paper, we will develop a fourth-order maximum principle preserving operator splitting method for solving the 2D and 3D space fractional Allen-Cahn equations (1.1). First, by using a second-order operator splitting method, at each time step, the numerical method is divided into three sub-steps. The first and third sub-steps involve the same ordinary differential equation (ODE), which can be solved analytically. The intermediate sub-step involves a 2D/3D space fractional diffusion equation, where the Crank-Nicolson scheme is adopted for time discretization, and the ADI method [6,16,18,36,42] combined with a fourth-order difference scheme is used for spatial discretization. The ADI technique converts the multidimensional space fractional diffusion problem into a series of one-dimensional problems, which greatly reduces the computational cost. The proposed method does not introduce any extra stabilized term and is shown to be unconditionally stable in L^2-norm by the Von Neumann stability analysis for second sub-step and a simple analysis for first and third sub-steps. The major contribution of this paper is to show that the temporal second-order accurate and spatial fourth-order accurate numerical solution satisfies the discrete maximum principle under the reasonable time step constraint. Numerical experiments are carried out for both 2D and 3D space fractional Allen-Cahn equations, the discrete maximum principle is well verified numerically. In addition, Richardson extrapolation is applied to increase the temporal accuracy to fourth-order. For fabricated smooth solutions, results confirm that the proposed method is unconditionally stable and fourth-order accurate for both time and space.

The organization of the paper is as follows. The operator splitting method for the 3D fractional Allen-Cahn equation is introduced in Section 2. The proof of the unconditional stability of the proposed method is given by Section 3. The discrete maximum principle is obtained in Section 4. Section 5 discusses Richardson extrapolation to obtain the fourth-order method both in time and space. Numerical results are provided in Section 6. And the conclusion is given in final section.

2. Numerical method

In the following, we will present the numerical method to solve the 3D space fractional Allen-Cahn equation. The difference scheme for the 2D case is similar but simpler.

For a positive integer N, let $\Delta t = T/N$, $t_n = n\Delta t$. The time domain $[0, T]$ is covered by $\{t_n\}$. Let s^n be the approximation of $s(x, y, z, n\Delta t)$ for an arbitrary function $s(x, y, z, t)$. The solution domain is defined as $\Omega \times [0, T]$ ($\Omega = [a, b]^3$), which is covered by a uniform grid $\Omega_h = \{(x_i, y_j, z_k, t_n)|x_i = ih_x, y_j = jh_y, z_k = kh_z, t_n = n\Delta t, i = 0, \cdots, M_x, j = 0, \cdots, M_y, k = 0, \cdots, M_z, n = 0, \cdots, N\}$, where $h_x = (b-a)/M_x, h_y = (b-a)/M_y, h_z = (b-a)/M_z$ and M_x, M_y, M_z are three positive integers. Let $U^n = (U^n_{i,j,k})_{(M_x+1)\times(M_y+1)\times(M_z+1)}$ be the numerical solution at time level $t = t_n$, the homogeneous Dirichlet boundary condition (1.3) gives

$$U^n_{0,j,k} = U^n_{M_x,j,k} = U^n_{i,0,k} = U^n_{i,M_y,k} = U^n_{i,j,0} = U^n_{i,j,M_z} = 0, \tag{2.1}$$

for any $n = 0, \cdots, N$. And the maximum norm of the numerical solution is denoted as

$$\|U^n\|_\infty = \max_{\substack{1\le i\le M_x-1\\ 1\le j\le M_y-1\\ 1\le k\le M_z-1}} |U^n_{i,j,k}|.$$

2.1. Temporal discretization

First, the space fractional Allen-Cahn equation (1.1) can be rewritten in the following form,

$$\frac{\partial u}{\partial t} = \mathcal{S}_1 u + \mathcal{S}_2 u, \tag{2.2}$$

where the operators $\mathcal{S}_1, \mathcal{S}_2$ are defined as

$$\mathcal{S}_1 u = u - u^3, \quad \mathcal{S}_2 u = \varepsilon^2 L_\alpha u.$$

According to Strang's second-order splitting method [41], the numerical solution of Eq. (2.2) in the time interval $[t_n, t_{n+1}]$ can be obtained as follows,

$$U^{n+1} = \left(\mathcal{S}_1^{\frac{\Delta t}{2}} \circ \mathcal{S}_2^{\Delta t} \circ \mathcal{S}_1^{\frac{\Delta t}{2}}\right) U^n, \tag{2.3}$$

where $\mathcal{S}_1^{\Delta t}$ and $\mathcal{S}_2^{\Delta t}$ are the evolution operators for $\frac{\partial u}{\partial t} = \mathcal{S}_1 u$ and $\frac{\partial u}{\partial t} = \mathcal{S}_2 u$, respectively.

More precisely, we can write the above splitting scheme (2.3) into three sub-steps as follows,

$$\frac{\partial \tilde{u}}{\partial t} = \frac{1}{2}(\tilde{u} - \tilde{u}^3), \quad \tilde{u}^n = U^n, \quad t \in [t_n, t_{n+1}], \tag{2.4}$$

$$\frac{\partial \bar{u}}{\partial t} = \varepsilon^2 L_\alpha \bar{u} = \varepsilon^2 \left(\mathcal{L}_x^\alpha \bar{u} + \mathcal{L}_y^\alpha \bar{u} + \mathcal{L}_z^\alpha \bar{u}\right), \quad \bar{u}^n = \tilde{u}^{n+1}, \quad t \in [t_n, t_{n+1}], \tag{2.5}$$

$$\frac{\partial \hat{u}}{\partial t} = \frac{1}{2}(\hat{u} - \hat{u}^3), \quad \hat{u}^n = \bar{u}^{n+1}, \quad t \in [t_n, t_{n+1}]. \tag{2.6}$$

The numerical solution at $t = t_{n+1}$ is given by $U^{n+1} = \hat{u}^{n+1}$.

The first and third sub-steps (2.4) and (2.6) involve the same ODE, which can be calculated analytically [24,49], i.e.,

$$\tilde{u}^{n+1} = \frac{U^n}{\sqrt{(U^n)^2 + \left(1-(U^n)^2\right)e^{-\Delta t}}}, \tag{2.7}$$

$$\hat{u}^{n+1} = \frac{\bar{u}^{n+1}}{\sqrt{(\bar{u}^{n+1})^2 + \left(1-(\bar{u}^{n+1})^2\right)e^{-\Delta t}}}. \tag{2.8}$$

The intermediate sub-step (2.5) involves solving a 3D space fractional diffusion equation. A Crank-Nicolson ADI method is used, which will be described in the following.

We first apply the Crank-Nicolson scheme for temporal discretization of Eq. (2.5), i.e.,

$$\frac{\bar{u}^{n+1}-\bar{u}^n}{\Delta t} = \varepsilon^2\left(\mathcal{L}_x^\alpha + \mathcal{L}_y^\alpha + \mathcal{L}_z^\alpha\right)\frac{\bar{u}^{n+1}+\bar{u}^n}{2} + O(\Delta t^2). \tag{2.9}$$

Collecting the terms for $\bar{u}^{n+1}$ and $\bar{u}^n$ in (2.9), one can get

$$\left(\frac{1}{\Delta t} - \frac{\varepsilon^2}{2}\left(\mathcal{L}_x^\alpha + \mathcal{L}_y^\alpha + \mathcal{L}_z^\alpha\right)\right)\bar{u}^{n+1} = \left(\frac{1}{\Delta t} + \frac{\varepsilon^2}{2}\left(\mathcal{L}_x^\alpha + \mathcal{L}_y^\alpha + \mathcal{L}_z^\alpha\right)\right)\bar{u}^n + O(\Delta t^2). \tag{2.10}$$

Eq. (2.10) is equivalent to

$$\begin{aligned}
&\frac{1}{\Delta t}\left(1-\frac{\Delta t\varepsilon^2}{2}\mathcal{L}_x^\alpha\right)\left(1-\frac{\Delta t\varepsilon^2}{2}\mathcal{L}_y^\alpha\right)\left(1-\frac{\Delta t\varepsilon^2}{2}\mathcal{L}_z^\alpha\right)\bar{u}^{n+1} \\
&= \frac{1}{\Delta t}\left(1+\frac{\Delta t\varepsilon^2}{2}\mathcal{L}_x^\alpha\right)\left(1+\frac{\Delta t\varepsilon^2}{2}\mathcal{L}_y^\alpha\right)\left(1+\frac{\Delta t\varepsilon^2}{2}\mathcal{L}_z^\alpha\right)\bar{u}^{n} \\
&+ \frac{\Delta t\varepsilon^4}{4}(\mathcal{L}_x^\alpha\mathcal{L}_y^\alpha + \mathcal{L}_x^\alpha\mathcal{L}_z^\alpha + \mathcal{L}_y^\alpha\mathcal{L}_z^\alpha)(\bar{u}^{n+1}-\bar{u}^n) - \frac{\Delta t^2\varepsilon^6}{8}\mathcal{L}_y^\alpha\mathcal{L}_x^\alpha\mathcal{L}_z^\alpha(\bar{u}^{n+1}+\bar{u}^n) + O(\Delta t^2).
\end{aligned} \tag{2.11}$$

Since

$$\begin{aligned}
&\frac{\Delta t\varepsilon^4}{4}(\mathcal{L}_x^\alpha\mathcal{L}_y^\alpha + \mathcal{L}_x^\alpha\mathcal{L}_z^\alpha + \mathcal{L}_y^\alpha\mathcal{L}_z^\alpha)(\bar{u}^{n+1}-\bar{u}^n) \\
&= \frac{\Delta t\varepsilon^4}{4}(\mathcal{L}_x^\alpha\mathcal{L}_y^\alpha + \mathcal{L}_x^\alpha\mathcal{L}_z^\alpha + \mathcal{L}_y^\alpha\mathcal{L}_z^\alpha)\left(\Delta t\frac{\partial \bar{u}^{n+\frac{1}{2}}}{\partial t} + O(\Delta t)^3\right) = O(\Delta t^2),
\end{aligned}$$

and

$$\frac{\Delta t^2\varepsilon^8}{8}\mathcal{L}_x^\alpha\mathcal{L}_z^\alpha\mathcal{L}_z^\alpha(u^{n+1}+u^n) = \frac{\Delta t^2\varepsilon^8}{8}\mathcal{L}_x^\alpha\mathcal{L}_y^\alpha\mathcal{L}_z^\alpha\left(2\bar{u}^{n+\frac{1}{2}} + O(\Delta t^2)\right) = O(\Delta t^2),$$

Eq. (2.11) is indeed

$$\begin{aligned}
&\frac{1}{\Delta t}\left(1-\frac{\Delta t\varepsilon^2}{2}\mathcal{L}_x^\alpha\right)\left(1-\frac{\Delta t\varepsilon^2}{2}\mathcal{L}_y^\alpha\right)\left(1-\frac{\Delta t\varepsilon^2}{2}\mathcal{L}_z^\alpha\right)\bar{u}^{n+1} \\
&= \frac{1}{\Delta t}\left(1+\frac{\Delta t\varepsilon^2}{2}\mathcal{L}_x^\alpha\right)\left(1+\frac{\Delta t\varepsilon^2}{2}\mathcal{L}_y^\alpha\right)\left(1+\frac{\Delta t\varepsilon^2}{2}\mathcal{L}_z^\alpha\right)\bar{u}^{n} + O(\Delta t^2).
\end{aligned} \tag{2.12}$$

The above discretization is only for time.

2.2. Spatial discretization

For spatial discretization, by using the homogenous boundary condition (2.1), the second-order difference scheme for the space fractional derivatives at internal point (x_i, y_j, z_k) is given as [4]

$$[\mathcal{L}_x^\alpha u]_{i,j,k} \approx -\frac{1}{h_x^\alpha}\sum_{s=i-M_x+1}^{i-1} c_s^\alpha u_{i-s,j,k} = -\frac{1}{h_x^\alpha}\sum_{s=1}^{M_x-1} c_{i-s}^\alpha u_{s,j,k}, \tag{2.13}$$

$$[\mathcal{L}_y^\alpha u]_{i,j,k} \approx -\frac{1}{h_y^\alpha}\sum_{s=j-M_y+1}^{j-1} c_s^\alpha u_{i,j-s,k} = -\frac{1}{h_y^\alpha}\sum_{s=1}^{M_y-1} c_{j-s}^\alpha u_{i,s,k}, \tag{2.14}$$

$$[\mathcal{L}_z^\alpha u]_{i,j,k} \approx -\frac{1}{h_z^\alpha}\sum_{s=k-M_z+1}^{k-1} c_s^\alpha u_{i,j,k-s} = -\frac{1}{h_z^\alpha}\sum_{s=1}^{M_z-1} c_{k-s}^\alpha u_{i,j,s}, \tag{2.15}$$

where

$$c_0^\alpha = \frac{\Gamma(\alpha+1)}{\left(\Gamma(\frac{\alpha}{2}+1)\right)^2}, \tag{2.16}$$

$$c_s^\alpha = \frac{(-1)^s\Gamma(\alpha+1)}{\Gamma(\frac{\alpha}{2}-s+1)\Gamma(\frac{\alpha}{2}+s+1)} = \left(1-\frac{\alpha+1}{\frac{\alpha}{2}+s}\right)c_{s-1}^\alpha, \quad \text{for } s\in\mathbb{Z}, \tag{2.17}$$

and $1 \le i \le M_x-1, 1 \le j \le M_y-1, 1 \le k \le M_z-1$.

Now we denote the operators $\Delta_x^\alpha, \Delta_y^\alpha, \Delta_z^\alpha$ and the identity operator I acting on the internal point (x_i, y_j, z_k) as follows,

$$[\Delta_x^\alpha u]_{i,j,k} = -\sum_{s=i-M_x+1}^{i-1} c_s^\alpha u_{i-s,j,k} = -\sum_{s=1}^{M_x-1} c_{i-s}^\alpha u_{s,j,k}, \tag{2.18}$$

$$[\Delta_y^\alpha u]_{i,j,k} = -\sum_{s=j-M_y+1}^{j-1} c_s^\alpha u_{i,j-s,k} = -\sum_{s=1}^{M_y-1} c_{j-s}^\alpha u_{i,s,k}, \tag{2.19}$$

$$[\Delta_z^\alpha u]_{i,j,k} = -\sum_{s=k-M_z+1}^{k-1} c_s^\alpha u_{i,j,k-s} = -\sum_{s=1}^{M_z-1} c_{k-s}^\alpha u_{i,j,s}, \tag{2.20}$$

and

$$[Iu]_{i,j,k} = u_{i,j,k}, \tag{2.21}$$

where $1 \le i \le M_x-1, 1 \le j \le M_y-1, 1 \le k \le M_z-1$.

Let $\mathcal{A}_x^\alpha, \mathcal{A}_y^\alpha, \mathcal{A}_z^\alpha$ be the average operators defined on the internal points (x_i, y_j, z_k) as [15]

$$\mathcal{A}_x^\alpha u_{i,j,k} = \frac{\alpha}{24}u_{i-1,j,k} + \left(1-\frac{\alpha}{12}\right)u_{i,j,k} + \frac{\alpha}{24}u_{i+1,j,k}, \tag{2.22}$$

$$\mathcal{A}_y^\alpha u_{i,j,k} = \frac{\alpha}{24}u_{i,j-1,k} + \left(1-\frac{\alpha}{12}\right)u_{i,j,k} + \frac{\alpha}{24}u_{i,j+1,k}, \tag{2.23}$$

$$\mathcal{A}_z^\alpha u_{i,j,k} = \frac{\alpha}{24}u_{i,j,k-1} + \left(1-\frac{\alpha}{12}\right)u_{i,j,k} + \frac{\alpha}{24}u_{i,j,k+1}, \tag{2.24}$$

where $1 \le i \le M_x-1, 1 \le j \le M_y-1, 1 \le k \le M_z-1$.

The fourth-order difference scheme for the space fractional derivatives at the internal point (x_i, y_j, z_k) is given as [15,17]

$$[\mathcal{L}_x^\alpha u]_{i,j,k} = \frac{1}{h_x^\alpha}[(\mathcal{A}_x^\alpha)^{-1}\Delta_x^\alpha u]_{i,j,k} + O(h_x^4), \tag{2.25}$$

$$[\mathcal{L}_y^\alpha u]_{i,j,k} = \frac{1}{h_y^\alpha}[(\mathcal{A}_y^\alpha)^{-1}\Delta_y^\alpha u]_{i,j,k} + O(h_y^4), \tag{2.26}$$

$$[\mathcal{L}_y^\alpha u]_{i,j,k} = \frac{1}{h_z^\alpha}[(\mathcal{A}_z^\alpha)^{-1}\Delta_z^\alpha u]_{i,j,k} + O(h_z^4), \tag{2.27}$$

where $1 \le i \le M_x-1, 1 \le j \le M_y-1, 1 \le k \le M_z-1$.

Substituting (2.25)-(2.27) into (2.12) and evaluating at the internal point (x_i, y_j, z_k), we have

$$\begin{aligned}
&\frac{1}{\Delta t}\left[\left(I-\frac{\Delta t\varepsilon^2}{2h_x^\alpha}(\mathcal{A}_x^\alpha)^{-1}\Delta_x^\alpha\right)\left(I-\frac{\Delta t\varepsilon^2}{2h_y^\alpha}(\mathcal{A}_y^\alpha)^{-1}\Delta_y^\alpha\right)\left(I-\frac{\Delta t\varepsilon^2}{2h_z^\alpha}(\mathcal{A}_z^\alpha)^{-1}\Delta_z^\alpha\right)\bar{u}^{n+1}\right]_{i,j,k} \\
&= \frac{1}{\Delta t}\left[\left(I+\frac{\Delta t\varepsilon^2}{2h_x^\alpha}(\mathcal{A}_x^\alpha)^{-1}\Delta_x^\alpha\right)\left(I+\frac{\Delta t\varepsilon^2}{2h_y^\alpha}(\mathcal{A}_y^\alpha)^{-1}\Delta_y^\alpha\right)\left(I+\frac{\Delta t\varepsilon^2}{2h_z^\alpha}(\mathcal{A}_z^\alpha)^{-1}\Delta_z^\alpha\right)\bar{u}^{n}\right]_{i,j,k} \\
&+ O(\Delta t^2 + h_x^4 + h_y^4 + h_z^4),
\end{aligned} \tag{2.28}$$

where $1 \le i \le M_x-1, 1 \le j \le M_y-1, 1 \le k \le M_z-1$.

Neglecting the truncation errors in (2.28), applying the operator $\mathcal{A}_x^\alpha\mathcal{A}_y^\alpha\mathcal{A}_z^\alpha$ to both sides and introducing the intermediate variables u^*, u^{**}, we obtain the D'Yakonov ADI-like scheme [36] as follows,

$$\left[(\mathcal{A}_x^\alpha - \beta_x\Delta_x^\alpha)\bar{u}^*\right]_{i,j,k} = \left[(\mathcal{A}_x^\alpha + \beta_x\Delta_x^\alpha)(\mathcal{A}_y^\alpha + \beta_y\Delta_y^\alpha)(\mathcal{A}_z^\alpha + \beta_z\Delta_z^\alpha)\bar{u}^n\right]_{i,j,k}, \tag{2.29}$$

$$\left[(\mathcal{A}_y^\alpha - \beta_y\Delta_y^\alpha)\bar{u}^{**}\right]_{i,j,k} = \bar{u}^*_{i,j,k}, \tag{2.30}$$

$$\left[(\mathcal{A}_z^\alpha - \beta_z\Delta_z^\alpha)\bar{u}^{n+1}\right]_{i,j,k} = \bar{u}^{**}_{i,j,k}, \tag{2.31}$$

where $\beta_x = \Delta t\varepsilon^2/(2h_x^\alpha)$, $\beta_y = \Delta t\varepsilon^2/(2h_y^\alpha)$, $\beta_z = \Delta t\varepsilon^2/(2h_z^\alpha)$ and $1 \le i \le M_x - 1, 1 \le j \le M_y - 1, 1 \le k \le M_z - 1$. Using the boundary condition (2.1), each of the above three equations is a one-dimensional linear system with homogeneous boundary conditions and all coefficient matrices are constant matrices whose inverse only need to be computed once during the whole computation. Thus, the above ADI method can be solved very efficiently.

Remark 1. From the analytical expression in (2.8) and homogeneous boundary condition (2.1), one can show that $\bar{u}^{n+1}$ also satisfies the homogeneous boundary condition since $U^{n+1} = \tilde{u}^{n+1}$ satisfies the homogeneous boundary condition. Thus, from above ADI scheme, one can see that $\bar{u}^{**}$ satisfies the homogeneous boundary condition in x, y directions and $\bar{u}^*$ satisfies the homogeneous boundary condition in x direction. These conditions are needed in the implementation of the above ADI scheme.

Remark 2. The above Crank-Nicolson ADI scheme (2.29)-(2.31) is second-order accurate in time and fourth-order accurate in space. Replacing the average operator $\mathcal{A}_x^\alpha$, $\mathcal{A}_y^\alpha$ and $\mathcal{A}_z^\alpha$ by the identity operator defined in (2.21), yields the following second-order scheme:

$$\left[(\mathcal{I} - \beta_x\Delta_x^\alpha)\bar{u}^*\right]_{i,j,k} = \left[(\mathcal{I} + \beta_x\Delta_x^\alpha)(\mathcal{I} + \beta_y\Delta_y^\alpha)(\mathcal{I} + \beta_z\Delta_z^\alpha)\bar{u}^n\right]_{i,j,k}, \tag{2.32}$$

$$\left[(\mathcal{I} - \beta_y\Delta_y^\alpha)\bar{u}^{**}\right]_{i,j,k} = \bar{u}^*_{i,j,k}, \tag{2.33}$$

$$\left[(\mathcal{I} - \beta_z\Delta_z^\alpha)\bar{u}^{n+1}\right]_{i,j,k} = \bar{u}^{**}_{i,j,k}, \tag{2.34}$$

where $1 \le i \le M_x - 1, 1 \le j \le M_y - 1, 1 \le k \le M_z - 1$.

3. Unconditional stability

In this section, we will first show that the first and third sub-steps in the splitting method (2.4)-(2.6) are unconditionally stable, then use von Neumann linear stability analysis to prove the unconditional stability of the ADI scheme (2.29)-(2.31) for the second sub-step when the exact solution u is smooth.

Lemma 1. *[4] The coefficients c_s^α have the following properties for $1 < \alpha \le 2$*

$$\begin{aligned} c_0^\alpha &= \frac{\Gamma(\alpha+1)}{\left(\Gamma(\frac{\alpha}{2}+1)\right)^2} > 0, \\ c_s^\alpha &= c_{-s}^\alpha \le 0, \quad \textit{for } s = \pm 1, \pm 2, \cdots, \\ \sum_{s=-M_{x(y,z)}+1+i, s\neq 0}^{i-1} |c_s^\alpha| &< c_0^\alpha, \quad \textit{for } i = 1, \cdots, M_{x(y,z)} - 1. \end{aligned} \tag{3.1}$$

Lemma 2. *Suppose that z is a complex number and $a > 0$ is a real number, then*

$$\left|\frac{a-z}{a+z}\right| \le 1 \quad \text{if and only if } \mathrm{Re}(z) \ge 0. \tag{3.2}$$

Proof. This lemma is easy to verify. $\square$

Lemma 3. *At any time level $t = t_n$, for any initial value $U^n_{i,j,k}(i = 0, \cdots, M_x, j = 0, \cdots, M_y, k = 0, \cdots, M_z)$, the numerical solution $\tilde{u}^{n+1}_{i,j,k}$ given by (2.7) for the first step (2.4) in the operator splitting method is unconditionally stable in L^∞-norm.*

Proof. For a given (i, j, k) $(i = 0, \cdots, M_x, j = 0, \cdots, M_y, k = 0, \cdots, M_z)$, there are following two cases.
Case 1. If the component $U^n_{i,j,k}$ satisfies $|U^n_{i,j,k}| \le 1$, then by using (2.7), one has

$$|\tilde{u}^{n+1}_{i,j,k}| = \frac{|U^n_{i,j,k}|}{\sqrt{(U^n_{i,j,k})^2 + \left(1 - (U^n_{i,j,k})^2\right)e^{-\Delta t}}} \le \frac{|U^n_{i,j,k}|}{\sqrt{(U^n_{i,j,k})^2}} = 1.$$

Case 2. If the component $U^n_{i,j,k}$ satisfies $|U^n_{i,j,k}| > 1$, then by using (2.7), one has

$$|\tilde{u}^{n+1}_{i,j,k}| = \frac{|U^n_{i,j,k}|}{\sqrt{(U^n_{i,j,k})^2(1 - e^{-\Delta t}) + e^{-\Delta t}}} \le \frac{|U^n_{i,j,k}|}{\sqrt{(1 - e^{-\Delta t}) + e^{-\Delta t}}} = |U^n_{i,j,k}|.$$

Combining these two cases, one has

$$\|\tilde{u}^{n+1}\|_\infty \le \max\left\{\|U^n\|_\infty, 1\right\},$$

which completes the proof of the lemma. □

Lemma 4. *At any time level $t = t_n$, for any initial value $\hat{u}^n_{i,j,k}(i = 0, \cdots, M_x, j = 0, \cdots, M_y, k = 0, \cdots, M_z)$, the numerical solution $\hat{u}^{n+1}_{i,j,k}$ given by (2.8) for the third step (2.6) in the operator splitting method is unconditionally stable in L^∞-norm.*

Proof. The proof of this lemma is similar as the proof of Lemma 3. □

Lemma 5. *The Crank-Nicolson ADI scheme (2.29)-(2.31) is unconditionally stable in L^2-norm.*

Proof. Let $\bar{u}^n_{i,j,k}$ be the numerical solution of the Crank-Nicolson ADI method (2.29)-(2.31). Since u is smooth with homogeneous boundary conditions, u can always be extended into a periodic function. Moreover, the first step (2.4) and the third step (2.6) is the same ODE, which are solved analytically. By induction, we can show that the numerical solution $\bar{u}^n_{i,j,k}$ at time level $t = t_n$ satisfy the homogenous boundary conditions and can be consider as the periodic grid function, which has the following discrete Fourier expansion form

$$\bar{u}^n_{i,j,k} = \sum_{p=0}^{M_x-1}\sum_{q=0}^{M_y-1}\sum_{r=0}^{M_z-1} \xi^n_{p,q,r} e^{I(ph_x i + qh_y j + rh_z k)}, \tag{3.3}$$

where $\xi^n_{p,q,r}$ are discrete Fourier coefficients at time level n, $I = \sqrt{-1}$ is the complex unit.

Since the numerical solution $\bar{u}^{n+1}_{i,j,k}$ at time level $t = t_{n+1}$ also satisfies the homogeneous boundary condition, it can be expressed as

$$\bar{u}^{n+1}_{i,j,k} = \sum_{p=0}^{M_x-1}\sum_{q=0}^{M_y-1}\sum_{r=0}^{M_z-1} \xi^{n+1}_{p,q,r} e^{I(ph_x i + qh_y j + rh_z k)}, \tag{3.4}$$

where $\xi^{n+1}_{p,q,r}$ are discrete Fourier coefficients at time level $n + 1$.

Substituting (3.3) into (2.29)-(2.31) and comparing the Fourier coefficients, one can get

$$\begin{aligned}\frac{\xi^{n+1}_{p,q,r}}{\xi^n_{p,q,r}} = &\left(\frac{1 + \frac{\alpha(\cos w_x - 1)}{12} - \beta_x \sum\limits_{s=p-M_x+1}^{p-1} c^\alpha_s e^{-Isw_x}}{1 + \frac{\alpha(\cos w_x - 1)}{12} + \beta_x \sum\limits_{s=p-M_x+1}^{p-1} c^\alpha_s e^{-Isw_x}}\right) \times \left(\frac{1 + \frac{\alpha(\cos w_y - 1)}{12} - \beta_y \sum\limits_{s=q-M_y+1}^{q-1} c^\alpha_s e^{-Isw_y}}{1 + \frac{\alpha(\cos w_y - 1)}{12} + \beta_y \sum\limits_{s=q-M_y+1}^{q-1} c^\alpha_s e^{-Isw_y}}\right) \\ &\times \left(\frac{1 + \frac{\alpha(\cos w_z - 1)}{12} - \beta_z \sum\limits_{s=t-M_z+1}^{t-1} c^\alpha_s e^{-Isw_z}}{1 + \frac{\alpha(\cos w_z - 1)}{12} + \beta_z \sum\limits_{s=t-M_z+1}^{t-1} c^\alpha_s e^{-Isw_z}}\right), \quad 0 \le p \le M_x - 1, \quad 0 \le q \le M_y - 1 \quad 0 \le t \le M_z - 1.\end{aligned} \tag{3.5}$$

From Lemma 1, we know that

$$\mathrm{Re}\left(\sum_{s=p-M_x+1}^{p-1} c^\alpha_s e^{-Isw_x}\right) = c^\alpha_0 + \sum_{s=p-M_x+1, s\ne 0}^{p-1} c^\alpha_s \cos(sw_x) \ge c^\alpha_0 - \sum_{s=p-M_x+1, s\ne 0}^{p-1} |c^\alpha_s| \ge 0.$$

Since $1 < \alpha \le 2$,

$$1 + \frac{\alpha(\cos w_x - 1)}{12} = \frac{12 + \alpha(\cos w_x - 1)}{12} \ge \frac{12 - 4}{12} > 0.$$

By using Lemma 2, one has

$$\left|\frac{1 + \frac{\alpha(\cos w_x - 1)}{12} - \beta_x \sum\limits_{s=i-M_x+1}^{i-1} c^\alpha_s e^{-Isw_x}}{1 + \frac{\alpha(\cos w_x - 1)}{12} + \beta_x \sum\limits_{s=i-M_x+1}^{i-1} c^\alpha_s e^{-Isw_x}}\right| \le 1. \tag{3.6}$$

Similarly, one has

$$\left| \frac{1 + \frac{\alpha(\cos w_y - 1)}{12} - \beta_y \sum\limits_{s=j-M_y+1}^{j-1} c_s^\alpha e^{-Isw_y}}{1 + \frac{\alpha(\cos w_y - 1)}{12} + \beta_y \sum\limits_{s=j-M_y+1}^{j-1} c_s^\alpha e^{-Isw_y}} \right| \leq 1, \tag{3.7}$$

and

$$\left| \frac{1 + \frac{\alpha(\cos w_z - 1)}{12} - \beta_z \sum\limits_{s=k-M_z+1}^{k-1} c_s^\alpha e^{-Isw_z}}{1 + \frac{\alpha(\cos w_z - 1)}{12} + \beta_z \sum\limits_{s=k-M_z+1}^{k-1} c_s^\alpha e^{-Isw_z}} \right| \leq 1. \tag{3.8}$$

Thus,

$$\left|\xi_{p,q,r}^{n+1}\right| \leq \left|\xi_{p,q,r}^{n}\right|, \quad 0 \leq p \leq M_x - 1, \quad 0 \leq q \leq M_y - 1 \quad 0 \leq t \leq M_z - 1. \tag{3.9}$$

Moreover, the Parseval's identity gives

$$\|\bar{u}^{n+1}\|_2^2 \triangleq h_x h_y h_z \sum_{i=0}^{M_x-1} \sum_{j=0}^{M_y-1} \sum_{k=0}^{M_z-1} \left|\bar{u}_{i,j,k}^{n+1}\right|^2 = \sum_{p=0}^{M_x-1} \sum_{q=0}^{M_y-1} \sum_{r=0}^{M_z-1} \left|\xi_{p,q,r}^{n+1}\right|^2 \tag{3.10}$$

and

$$\|\bar{u}^{n}\|_2^2 \triangleq h_x h_y h_z \sum_{i=0}^{M_x-1} \sum_{j=0}^{M_y-1} \sum_{k=0}^{M_z-1} \left|\bar{u}_{i,j,k}^{n}\right|^2 = \sum_{p=0}^{M_x-1} \sum_{q=0}^{M_y-1} \sum_{r=0}^{M_z-1} \left|\xi_{p,q,r}^{n}\right|^2 \tag{3.11}$$

Therefore,

$$\|\bar{u}^{n+1}\|_2 \leq \|\bar{u}^{n}\|_2. \tag{3.12}$$

This completes the proof of the lemma. □

Theorem 1. *The operator splitting scheme (2.4), (2.29)-(2.31) and (2.6) is unconditionally stable in L^2-norm.*

Proof. Combining the results of Lemma 3, 4, 5 gives the result. □

4. Discrete maximum principle

Lemma 6. *Let matrix $\mathbf{C}_x$ be defined as follows:*

$$\mathbf{C}_x = \begin{pmatrix} -c_0^\alpha & 0 & \cdots & \cdots & \cdots & 0 & 0 \\ -c_1^\alpha & -c_0^\alpha & -c_{-1}^\alpha & \cdots & \cdots & -c_{-M_x+2}^\alpha & -c_{-M_x+1}^\alpha \\ -c_2^\alpha & -c_1^\alpha & -c_0^\alpha & -c_{-1}^\alpha & \cdots & \cdots & -c_{-M_x+2}^\alpha \\ \vdots & \ddots & \ddots & \ddots & \ddots & \ddots & \vdots \\ -c_{M_x-2}^\alpha & \vdots & \ddots & \ddots & \ddots & \ddots & -c_{-2}^\alpha \\ -c_{M_x-1}^\alpha & -c_{M_x-2}^\alpha & \cdots & \cdots & -c_1^\alpha & -c_0^\alpha & -c_{-1}^\alpha \\ 0 & 0 & \cdots & \cdots & 0 & 0 & -c_0^\alpha \end{pmatrix}_{(M_x+1)\times(M_x+1)}. \tag{4.1}$$

Then, $\mathbf{C}_x$ is strictly diagonally dominant [4], i.e.

$$|c_{ii}| = c_0^\alpha > \sum_{j\neq i} |c_{ij}|, \quad \text{for } i = 1, \cdots, M_x + 1. \tag{4.2}$$

Similarly, we can define $(M_y + 1) \times (M_y + 1)$ square matrix $\mathbf{C}_y$ and $(M_z + 1) \times (M_z + 1)$ square matrix $\mathbf{C}_z$, which are also strictly diagonally dominant.

Lemma 7. *[38,43] Let matrix* $\mathbf{B} \in \mathbb{R}^{(M+1)\times(M+1)}$, $\mathbf{A} = a\mathbf{I} - \mathbf{B}$, *where* $a > 0$, $\mathbf{I}$ *is the identity matrix with same size of* $\mathbf{B}$ *and* $\mathbf{B}$ *is a negative diagonally dominant matrix, i.e.*

$$\forall\, i = 1, \cdots, M+1, \quad b_{ii} \le 0, \quad \text{and} \quad b_{ii} + \sum_{j\neq i} |b_{ij}| \le 0,$$

then $\mathbf{A}$ *is invertible and*

$$\|\mathbf{A}^{-1}\|_\infty \le \frac{1}{a}. \tag{4.3}$$

In the section, we will show that, under certain reasonable time step constraint, the discrete maximum principle for the proposed method is valid.

Theorem 2. *Assume that the initial value* $u_0(x)$ *satisfies* $\max_{x\in\bar\Omega} |u_0(x)| \le 1$, *then the numerical solution* $U^n_{i,j,k}$ *of (2.4), (2.29)-(2.31) and (2.6) satisfies the discrete maximum principle, i.e.,* $\|U^n\|_\infty \le 1$ *for any* $n = 0, 1, \cdots, N$ *if the time step* Δt *satisfies*

$$\frac{\alpha+2}{12}\frac{\max(h_x^\alpha, h_y^\alpha, h_z^\alpha)}{\varepsilon^2 c_0^\alpha} \le \Delta t \le \frac{12-\alpha}{6}\frac{\min(h_x^\alpha, h_y^\alpha, h_z^\alpha)}{\varepsilon^2 c_0^\alpha}. \tag{4.4}$$

Proof. We prove the theorem by mathematical induction. Obviously, $\|U^n\|_\infty \le 1$ for $n = 0$ since $U^0_{i,j,k} = u_0(x_i, y_j, z_k)$. Assume that $\|U^k\|_\infty \le 1$ $(k \le n)$ is valid, we want to show that $\|U^{n+1}\|_\infty \le 1$. From (2.7) and the proof of Lemma 3, one can easily obtain that

$$\|\tilde u^{n+1}\|_\infty \le 1. \tag{4.5}$$

Next, we look at the numerical solution $\bar u^{n+1}$ of (2.29)-(2.31). Since $\bar u^n = \tilde u^{n+1}$, one has

$$\|\bar u^n\|_\infty \le 1. \tag{4.6}$$

Let $\bar u^n = (\bar u^n_{i,j,k})_{(M_x+1)\times(M_y+1)\times(M_z+1)}$ be a 3D matrix including the boundary points, which are zero values. Denfine matrix $\mathbf{D}_x$ as follows

$$\mathbf{D}_x = \begin{pmatrix} -2 & 0 & 0 & \cdots & \cdots & 0 \\ 1 & -2 & 1 & 0 & \cdots & 0 \\ 0 & 1 & -2 & 1 & \ddots & 0 \\ \vdots & \ddots & \ddots & \ddots & \ddots & \vdots \\ 0 & \cdots & 0 & 1 & -2 & 1 \\ 0 & \cdots & 0 & 0 & 0 & -2 \end{pmatrix}_{(M_x+1)\times(M_x+1)}. \tag{4.7}$$

Another two square matrices $\mathbf{D}_y$ and $\mathbf{D}_z$ can be defined similarly.

From the definition of the operators $\Delta_x^\alpha, \Delta_y^\alpha, \Delta_z^\alpha, I$ in (2.18)-(2.21) and the zero value on boundary points, one can see that the application of operator $\mathcal{A}_z^\alpha + \beta_z\Delta_z^\alpha$ to $\bar u^n$ is equivalent to multiply each vector in the third dimension of $\bar u^n$ by the matrix $\mathbf{I}_z + \frac{\alpha}{24}\mathbf{D}_z + \beta_z\mathbf{C}_z$ ($\mathbf{I}_z$ is the identity matrix with size $(M_z+1)\times(M_z+1)$), the application of operator $\mathcal{A}_y^\alpha + \beta_y\Delta_y^\alpha$ to $\bar u^n$ is equivalent to multiply each vector in the second dimension of $\bar u^n$ by the matrix $\mathbf{I}_y + \frac{\alpha}{24}\mathbf{D}_y + \beta_y\mathbf{C}_y$ ($\mathbf{I}_y$ is the identity matrix with size $(M_y+1)\times(M_y+1)$), and the application of operator $\mathcal{A}_x^\alpha + \beta_x\Delta_x^\alpha$ to $\bar u^n$ is equivalent to multiply each vector in the first dimension of $\bar u^n$ by the matrix $\mathbf{I}_x + \frac{\alpha}{24}\mathbf{D}_x + \beta_x\mathbf{C}_x$ ($\mathbf{I}_x$ is the identity matrix with size $(M_x+1)\times(M_x+1)$).

In addition, (2.29)-(2.31) is equivalent to

$$\left[\left(\mathcal{A}_x^\alpha - \beta_x\Delta_x^\alpha\right)\left(\mathcal{A}_y^\alpha - \beta_y\Delta_y^\alpha\right)\left(\mathcal{A}_z^\alpha - \beta_z\Delta_z^\alpha\right)\bar u^{n+1}\right]_{i,j,k} = \left[\left(\mathcal{A}_x^\alpha + \beta_x\Delta_x^\alpha\right)\left(\mathcal{A}_y^\alpha + \beta_y\Delta_y^\alpha\right)\left(\mathcal{A}_z^\alpha + \beta_z\Delta_z^\alpha\right)\bar u^{n}\right]_{i,j,k}, \tag{4.8}$$

which further yields

$$\bar u^{n+1}_{i,j,k} = \left[\left(\mathcal{A}_z^\alpha - \beta_z\Delta_z^\alpha\right)^{-1}\left(\mathcal{A}_y^\alpha - \beta_y\Delta_y^\alpha\right)^{-1}\left(\mathcal{A}_x^\alpha - \beta_x\Delta_x^\alpha\right)^{-1}\left(\mathcal{A}_x^\alpha + \beta_x\Delta_x^\alpha\right)\left(\mathcal{A}_y^\alpha + \beta_y\Delta_y^\alpha\right)\left(\mathcal{A}_z^\alpha + \beta_z\Delta_z^\alpha\right)\bar u^{n}\right]_{i,j,k}, \tag{4.9}$$

where the application of operator $(\mathcal{A}_z^\alpha - \beta_z\Delta_z^\alpha)^{-1}$ to a 3D matrix is equivalent to multiply each vector in the third dimension of this 3D matrix by the matrix $(\mathbf{I}_z + \frac{\alpha}{24}\mathbf{D}_z - \beta_z\mathbf{C}_z)^{-1}$, the application of operator $(\mathcal{A}_y^\alpha - \beta_y\Delta_y^\alpha)^{-1}$ to a 3D matrix is equivalent to multiply each vector in the second dimension of this 3D matrix by the matrix $(\mathbf{I}_y + \frac{\alpha}{24}\mathbf{D}_y - \beta_y\mathbf{C}_y)^{-1}$, and the application of operator $(\mathcal{A}_x^\alpha - \beta_x\Delta_x^\alpha)^{-1}$ to a 3D matrix is equivalent to multiply each vector in the first dimension of this 3D matrix by the matrix $(\mathbf{I}_x + \frac{\alpha}{24}\mathbf{D}_x - \beta_x\mathbf{C}_x)^{-1}$.

Therefore, it is easy to check that $\bar{u}^{n+1} = (\bar{u}^{n+1}_{i,j,k})_{(M_x+1)\times(M_y+1)\times(M_z+1)}$ can be obtained from $\bar{u}^n = (\bar{u}^n_{i,j,k})_{(M_x+1)\times(M_y+1)\times(M_z+1)}$ through a series of one-dimensional vector transformations as follows:

(i) Multiplying each vector in the third dimension of $\bar{u}^n$ by the matrix $\mathbf{I}_z + \frac{\alpha}{24}\mathbf{D}_z + \beta_z\mathbf{C}_z$,
(ii) Multiplying each vector in the second dimension of resulting matrix in (i) by the matrix $\mathbf{I}_y + \frac{\alpha}{24}\mathbf{D}_y + \beta_y\mathbf{C}_y$,
(iii) Multiplying each vector in the first dimension of resulting matrix in (ii) by the matrix $\mathbf{I}_x + \frac{\alpha}{24}\mathbf{D}_x + \beta_x\mathbf{C}_x$,
(iv) Multiplying each vector in the first dimension of resulting matrix in (iii) by the matrix $(\mathbf{I}_x + \frac{\alpha}{24}\mathbf{D}_x - \beta_x\mathbf{C}_x)^{-1}$,
(v) Multiplying each vector in the second dimension of resulting matrix in (iv) by the matrix $(\mathbf{I}_y + \frac{\alpha}{24}\mathbf{D}_y - \beta_y\mathbf{C}_y)^{-1}$,
(vi) Multiplying each vector in the third dimension of resulting matrix in (v) by the matrix $(\mathbf{I}_z + \frac{\alpha}{24}\mathbf{D}_z - \beta_z\mathbf{C}_z)^{-1}$.

If condition (4.4) is satisfied, then

$$1 - \frac{\alpha}{12} - \beta_z c_0^\alpha > 0, \tag{4.10}$$

and

$$\sum_j \left|\delta_{i,j} + \frac{\alpha}{24}d_{i,j} + \beta_z c_{i,j}\right| = 1 - \frac{\alpha}{12} - \beta_z c_0^\alpha < 1, \quad \text{for} \quad i = 1, M_z + 1, \tag{4.11}$$

$$\begin{aligned}\sum_j \left|\delta_{i,j} + \frac{\alpha}{24}d_{i,j} + \beta_z c_{i,j}\right| &\le 1 - \frac{\alpha}{12} - \beta_z c_0^\alpha + \frac{\alpha}{24} + \frac{\alpha}{24} + \beta_z \sum_{j\neq i}\left|c_{i,j}\right| \\ &= 1 - \beta_z\left(c_0^\alpha - \sum_{j\neq i}|c_{i,j}|\right) \\ &< 1, \qquad \text{for} \quad i = 2, \cdots, M_z.\end{aligned} \tag{4.12}$$

Thus,

$$\left\|\mathbf{I}_z + \frac{\alpha}{24}\mathbf{D}_z + \beta_z\mathbf{C}_z\right\|_\infty < 1. \tag{4.13}$$

By using (4.6) and (4.13), one gets

$$\left\|\left(\mathcal{A}_z^\alpha + \beta_z\Delta_z^\alpha\right)\bar{u}^n\right\|_\infty \le \left\|\mathbf{I}_z + \frac{\alpha}{24}\mathbf{D}_z + \beta_z\mathbf{C}_z\right\|_\infty \cdot \|\bar{u}^n\|_\infty \le 1. \tag{4.14}$$

Similarly,

$$\left\|\mathbf{I}_y + \frac{\alpha}{24}\mathbf{D}_y + \beta_y\mathbf{C}_y\right\|_\infty < 1, \quad \left\|\mathbf{I}_x + \frac{\alpha}{24}\mathbf{D}_x + \beta_x\mathbf{C}_x\right\|_\infty < 1. \tag{4.15}$$

Therefore,

$$\left\|\left(\mathcal{A}_y^\alpha + \beta_y\Delta_y^\alpha\right)\left(\mathcal{A}_z^\alpha + \beta_z\Delta_z^\alpha\right)\bar{u}^n\right\|_\infty \le 1, \tag{4.16}$$

and

$$\left\|\left(\mathcal{A}_x^\alpha + \beta_x\Delta_x^\alpha\right)\left(\mathcal{A}_y^\alpha + \beta_y\Delta_y^\alpha\right)\left(\mathcal{A}_z^\alpha + \beta_z\Delta_z^\alpha\right)\bar{u}^n\right\|_\infty \le 1. \tag{4.17}$$

If condition (4.4) is satisfied, then

$$\frac{\alpha}{12} - \beta_x c_0^\alpha = \frac{\alpha}{12} - \frac{\Delta t\varepsilon^2}{2h_x^\alpha}c_0^\alpha \le 0, \tag{4.18}$$

$$-\frac{\alpha}{24} - \beta_x c_1^\alpha = -\frac{\alpha}{24} - \frac{\Delta t\varepsilon^2}{2h_x^\alpha}(1 - \frac{\alpha+1}{\frac{\alpha}{2}+1})c_0^\alpha = -\frac{\alpha}{24} + \frac{\Delta t\varepsilon^2}{2h_x^\alpha}\frac{\alpha}{\alpha+2}c_0^\alpha \ge 0, \tag{4.19}$$

where Eq. (2.17) is used.

Now for matrix $-\frac{\alpha}{24}\mathbf{D}_x + \beta_x\mathbf{C}_x$, one has

$$\sum_{j\neq i}\left|-\frac{\alpha}{24}d_{i,j} + \beta_x c_{i,j}\right| = 0 \le -\frac{\alpha}{12} + \beta_x c_0^\alpha = -\left(-\frac{\alpha}{24}d_{i,i} + \beta_x c_{i,i}\right), \quad \text{for} \quad i = 1, M_x + 1, \tag{4.20}$$

and

$$
\begin{aligned}
\sum_{j\neq i}\left|-\frac{\alpha}{24}d_{i,j}+\beta_x c_{i,j}\right| &= \sum_{j\neq i,i\pm1}\left|-\frac{\alpha}{24}d_{i,j}+\beta_x c_{i,j}\right|+(-\frac{\alpha}{24}-\beta_x c_1^{\alpha})+(-\frac{\alpha}{24}-\beta_x c_{-1}^{\alpha}),\\
&=-\frac{\alpha}{12}+\sum_{j\neq i,i\pm1}\beta_x\left|c_{i,j}\right|+(-\beta_x c_1^{\alpha})+(-\beta_x c_{-1}^{\alpha})\\
&=-\frac{\alpha}{12}+\sum_{j\neq i}\beta_x\left|c_{i,j}\right|\\
&\leq -\frac{\alpha}{12}+\beta_x\left|c_{i,i}\right|\\
&=-\frac{\alpha}{12}+\beta_x c_0^{\alpha}\\
&=-\left(-\frac{\alpha}{24}d_{i,i}+\beta_x c_{i,i}\right), \qquad \text{for} \quad i=2,\cdots,M_x.
\end{aligned}
\tag{4.21}
$$

Thus, $-\frac{\alpha}{24}\mathbf{D}_x+\beta_x\mathbf{C}_x$ is a negative diagonally dominant matrix. By using Lemma 7, one has

$$
\left\|\left(\mathbf{I}_x+\frac{\alpha}{24}\mathbf{D}_x-\beta_x\mathbf{C}_x\right)^{-1}\right\|_{\infty}\leq 1. \tag{4.22}
$$

Applying the above condition and using (4.17), one has

$$
\left\|\left(\mathcal{A}_x^{\alpha}-\beta_x\Delta_x^{\alpha}\right)^{-1}\left(\mathcal{A}_x^{\alpha}+\beta_x\Delta_x^{\alpha}\right)\left(\mathcal{A}_y^{\alpha}+\beta_y\Delta_y^{\alpha}\right)\left(\mathcal{A}_z^{\alpha}+\beta_z\Delta_z^{\alpha}\right)\bar{u}^n\right\|_{\infty}\leq 1. \tag{4.23}
$$

Similarly, if condition (4.4) is satisfied, one has

$$
\left\|\left(\mathbf{I}_y+\frac{\alpha}{24}\mathbf{D}_y-\beta_y\mathbf{C}_y\right)^{-1}\right\|_{\infty}\leq 1, \quad \left\|\left(\mathbf{I}_z+\frac{\alpha}{24}\mathbf{D}_z-\beta_z\mathbf{C}_z\right)^{-1}\right\|_{\infty}\leq 1. \tag{4.24}
$$

Thus,

$$
\left\|\left(\mathcal{A}_y^{\alpha}-\beta_y\Delta_y^{\alpha}\right)^{-1}\left(\mathcal{A}_x^{\alpha}-\beta_x\Delta_x^{\alpha}\right)^{-1}\left(\mathcal{A}_x^{\alpha}+\beta_x\Delta_x^{\alpha}\right)\left(\mathcal{A}_y^{\alpha}+\beta_y\Delta_y^{\alpha}\right)\left(\mathcal{A}_z^{\alpha}+\beta_z\Delta_z^{\alpha}\right)\bar{u}^n\right\|_{\infty}\leq 1, \tag{4.25}
$$

and

$$
\left\|\left(\mathcal{A}_z^{\alpha}-\beta_z\Delta_z^{\alpha}\right)^{-1}\left(\mathcal{A}_y^{\alpha}-\beta_y\Delta_y^{\alpha}\right)^{-1}\left(\mathcal{A}_x^{\alpha}-\beta_x\Delta_x^{\alpha}\right)^{-1}\left(\mathcal{A}_x^{\alpha}+\beta_x\Delta_x^{\alpha}\right)\left(\mathcal{A}_y^{\alpha}+\beta_y\Delta_y^{\alpha}\right)\left(\mathcal{A}_z^{\alpha}+\beta_z\Delta_z^{\alpha}\right)\bar{u}^n\right\|_{\infty}\leq 1. \tag{4.26}
$$

This yields

$$
\left\|\bar{u}^{n+1}\right\|_{\infty}\leq 1. \tag{4.27}
$$

Finally, from (2.8) and Lemma 4, one can obtain that

$$
\|\hat{u}^{n+1}\|_{\infty}\leq 1. \tag{4.28}
$$

Thus,

$$
\|U^{n+1}\|_{\infty}=\|\hat{u}^{n+1}\|_{\infty}\leq 1. \tag{4.29}
$$

This completes the proof of the theorem. □

Remark 3. The first entry in the first row and the last entry in the last row in both matrices $\mathbf{C}_{x(y,z)}$ and $\mathbf{D}_{x(y,z)}$ can take arbitrary numbers due to homogeneous Dirichlet boundary conditions. Here we set these two elements the same as the diagonal entry of matrices $\mathbf{C}_{x(y,z)}$ and $\mathbf{D}_{x(y,z)}$ so that Lemma 7 can be directly applied when obtaining the estimate (4.22).

Remark 4. Lemma 3 to Lemma 5 indicate the numerical solution of the proposed scheme is bounded in L^2-norm without any time step constraint while the discrete maximum principle of the numerical solution in L^{∞}-norm is valid when the time step size satisfies (4.4).

The theoretical results in previous sections also hold for the second-order scheme (2.4), (2.32)-(2.34) and (2.6) with some minor changes. For example, Theorem 2 will become the following theorem.

Theorem 3. *Assume that the initial value $u_0(x)$ satisfies $\max_{x\in\bar{\Omega}} |u_0(x)| \le 1$, then the numerical solution $U^n_{i,j,k}$ of (2.4), (2.32)-(2.34) and (2.6) satisfies the discrete maximum principle, i.e., $\|U^n\|_\infty \le 1$ for any $n = 0, 1, \cdots, N$ if the time step Δt satisfies*

$$\Delta t \le 2\frac{\min(h_x^\alpha, h_y^\alpha, h_z^\alpha)}{\varepsilon^2 c_0^\alpha}. \tag{4.30}$$

Proof. The main difference from Theorem 2 is that the matrices $\mathbf{D}_x$, $\mathbf{D}_y$ and $\mathbf{D}_z$ should be changed into zero matrices. Other parts of the proof are basically the same as Theorem 2. □

5. Richardson extrapolation to obtain fourth-order accuracy

Since the temporal order of accuracy of the ADI scheme (2.29)–(2.31) is two, which is the same as the Strang's time splitting method (2.4)–(2.6). Consequently, the proposed operator splitting method (2.4)–(2.6) together with the ADI scheme (2.29)–(2.31) will be second-order accurate in time and fourth-order accurate in space. In order to increase the time accuracy, we apply the following Richardson extrapolation for the numerical solution at the final time step:

$$\widetilde{U} = \frac{4}{3}U(\Delta t, h_x, h_y, h_z) - \frac{1}{3}U(2\Delta t, h_x, h_y, h_z), \tag{5.1}$$

where $U(\Delta t, h_x, h_y, h_z)$, $U(2\Delta t, h_x, h_y, h_z)$ are numerical solutions at the final time step $t = T$ by using spatial meshsizes h_x, h_y, h_z and time steps Δt, $2\Delta t$, respectively.

If the exact solution has sufficient regularity, then the extrapolated solution $\widetilde{U}$ is fourth-order accurate in both time and space, see last two columns of Tables 1–10 in the next section for details.

6. Numerical results

Our code is written in Matlab and programs are carried out on a desktop with Intel CPU i7-4790 K (4.00 GHz) and 16 GB RAM.

6.1. Convergence and stability study

In order to numerically test the accuracy of the numerical method, we use exact solutions with sufficient regularity in this subsection as the testing examples.

Example 1. In this example, we consider the 2D space fractional Allen-Cahn equation with the exact solution

$$u(x, y, t) = e^{-t}x^4(1-x)^4y^4(1-y)^4, \tag{6.1}$$

so that the exact solution has a sufficient regularity. And in this example, the equation needs to be modified with a source term

$$\begin{aligned}
f(x, y, t) = {} & \frac{\varepsilon^2}{2\cos(\frac{\alpha\pi}{2})}e^{-t}\Big[\frac{\Gamma(5)}{\Gamma(5-\alpha)}(x^{4-\alpha} + (1-x)^{4-\alpha}) - \frac{4\Gamma(6)}{\Gamma(6-\alpha)}(x^{5-\alpha} + (1-x)^{5-\alpha}) \\
& + \frac{6\Gamma(7)}{\Gamma(7-\alpha)}(x^{6-\alpha} + (1-x)^{6-\alpha}) - \frac{4\Gamma(8)}{\Gamma(8-\alpha)}(x^{7-\alpha} + (1-x)^{7-\alpha}) \\
& + \frac{\Gamma(9)}{\Gamma(9-\alpha)}(x^{8-\alpha} + (1-x)^{8-\alpha})\Big]y^4(1-y)^4 \\
& + \frac{\varepsilon^2}{2\cos(\frac{\alpha\pi}{2})}e^{-t}\Big[\frac{\Gamma(5)}{\Gamma(5-\alpha)}(y^{4-\alpha} + (1-y)^{4-\alpha}) - \frac{4\Gamma(6)}{\Gamma(6-\alpha)}(y^{5-\alpha} + (1-y)^{5-\alpha}) \\
& + \frac{6\Gamma(7)}{\Gamma(7-\alpha)}(y^{6-\alpha} + (1-y)^{6-\alpha}) - \frac{4\Gamma(8)}{\Gamma(8-\alpha)}(y^{7-\alpha} + (1-y)^{7-\alpha}) \\
& + \frac{\Gamma(9)}{\Gamma(9-\alpha)}(y^{8-\alpha} + (1-y)^{8-\alpha})\Big]x^4(1-x)^4 \\
& + e^{-3t}x^{12}(1-x)^{12}y^{12}(1-y)^{12} - 2e^{-t}x^4(1-x)^4y^4(1-y)^4.
\end{aligned}$$

The initial condition is given according to this exact solution and ε is set to be 0.1.

Table 1
L^∞-norm errors and CPU times (in seconds) for Example 1 with $\alpha = 1.2$.

Δt	h	CPU	$\parallel e_1 \parallel_\infty$	order$_1$	$\parallel e_2 \parallel_\infty$	order$_2$
1/16	1/16	0.02s	1.79E−08		5.45E−10	
1/32	1/32	0.07s	4.37E−09	2.03	3.41E−11	4.00
1/64	1/64	0.23s	1.09E−09	2.01	4.19E−12	3.02
1/128	1/128	0.98s	2.71E−10	2.00	3.27E−13	3.68
1/256	1/256	7.44s	6.78E−11	2.00	2.50E−14	3.71

Table 2
L^∞-norm errors and CPU times (in seconds) for Example 1 with $\alpha = 1.5$.

Δt	h	CPU	$\parallel e_1 \parallel_\infty$	order$_1$	$\parallel e_2 \parallel_\infty$	order$_2$
1/16	1/16	0.02s	1.48E−08		1.04E−09	
1/32	1/32	0.07s	3.51E−09	2.08	6.48E−11	4.00
1/64	1/64	0.23s	8.66E−10	2.02	4.06E−12	4.00
1/128	1/128	0.97s	2.16E−10	2.00	2.54E−13	4.00
1/256	1/256	7.43s	5.39E−11	2.00	1.72E−14	3.88

Table 3
L^∞-norm errors and CPU times (in seconds) for Example 1 with $\alpha = 1.8$.

Δt	h	CPU	$\parallel e_1 \parallel_\infty$	order$_1$	$\parallel e_2 \parallel_\infty$	order$_2$
1/16	1/16	0.02s	1.08E−08		1.96E−09	
1/32	1/32	0.06s	2.37E−09	2.19	1.17E−10	4.06
1/64	1/64	0.23s	5.71E−10	2.05	7.03E−12	4.06
1/128	1/128	0.97s	1.41E−10	2.01	4.30E−13	4.03
1/256	1/256	7.43s	3.53E−11	2.00	2.69E−14	4.00

Table 4
L^∞-norm errors and CPU times (in seconds) for Example 1 with $\alpha = 2.0$.

Δt	h	CPU	$\parallel e_1 \parallel_\infty$	order$_1$	$\parallel e_2 \parallel_\infty$	order$_2$
1/16	1/16	0.02s	7.94E−09		2.88E−09	
1/32	1/32	0.06s	1.56E−09	2.34	1.80E−10	3.99
1/64	1/64	0.23s	3.78E−10	2.05	1.13E−11	4.00
1/128	1/128	0.97s	9.39E−11	2.01	7.06E−13	4.00
1/256	1/256	7.43s	2.35E−11	2.00	4.42E−14	4.00

Table 5
L^∞-norm errors and CPU times (in seconds) for Example 1 with $\alpha = 1.5$ using unequal meshsizes in x and y directions.

Δt	h_x	h_y	CPU	$\parallel e_1 \parallel_\infty$	order$_1$	$\parallel e_2 \parallel_\infty$	order$_2$
1/16	1/16	1/32	0.03s	1.43E−08		9.83E−09	
1/32	1/32	1/64	0.10s	3.48E−09	2.04	5.89E−11	4.06
1/64	1/64	1/128	0.29s	8.64E−10	2.01	3.63E−12	4.02
1/128	1/128	1/256	1.94s	2.16E−10	2.00	2.22E−13	4.03
1/256	1/256	1/512	17.0s	5.39E−11	2.00	1.72E−14	3.69

We carry out numerical accuracy test for $1 < \alpha \leq 2$. We measure the numerical errors $e_1(\Delta t, h_x, h_y, h_z) = u - U(\Delta t, h_x, h_y, h_z)$ and $e_2(\Delta t, h_x, h_y, h_z) = u - \widetilde{U}(\Delta t, h_x, h_y, h_z)$ at time $T = 1$ in the L^∞-norm, and compute the convergence orders according to

$$\text{order}_1 = \log_2\left(\frac{\parallel e_1(\Delta t, h_x, h_y, h_z) \parallel_\infty}{\parallel e_1(\Delta t/2, h_x/2, h_y/2, h_z/2) \parallel_\infty}\right),$$

and

$$\text{order}_2 = \log_2\left(\frac{\parallel e_2(\Delta t, h_x, h_y, h_z) \parallel_\infty}{\parallel e_2(\Delta t/2, h_x/2, h_y/2, h_z/2) \parallel_\infty}\right).$$

Table 1-Table 4 list the errors and the corresponding convergence orders for $\alpha = 1.2, 1.5, 1.8, 2$ in the L^∞-norm using the same spatial meshsize $h = h_x = h_y$ while Table 5 lists the errors and the corresponding convergence orders for $\alpha = 1.5$ in the L^∞-norm using different spatial meshsizes. As we can see that these results confirm second-order accuracy in time variable and fourth-order accuracy in space variable if the Richardson extrapolation (5.1) is not applied. But the results

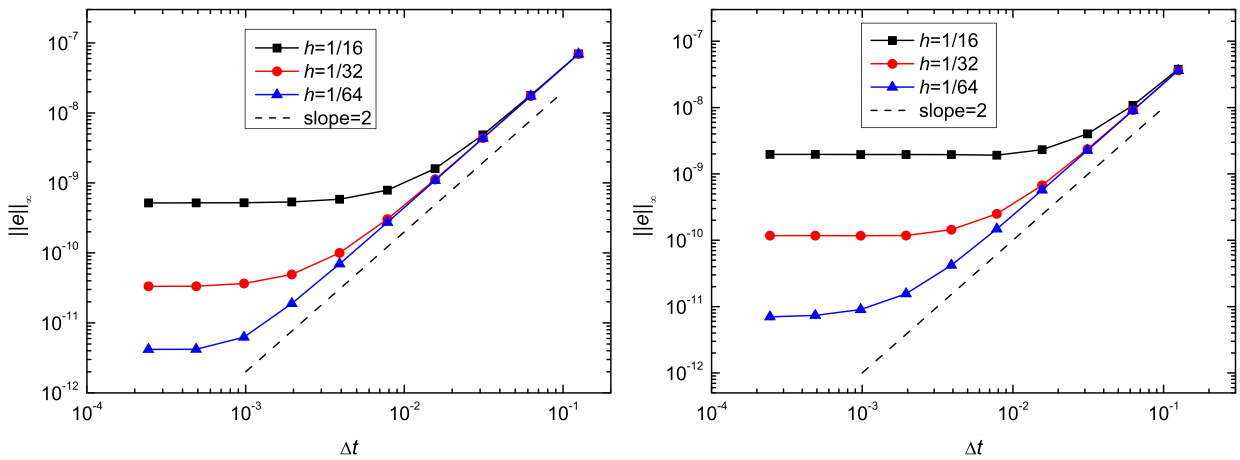

(a) $\alpha = 1.2$ (b) $\alpha = 1.8$

Fig. 1. Numerical results for Example 1 with fixed h but varying Δt.

Table 6
L^∞-norm errors and CPU times (in seconds) for Example 2 with $\alpha = 1.2$.

Δt	h	CPU	$\| e_1 \|_\infty$	order$_1$	$\| e_2 \|_\infty$	order$_2$
1/8	1/8	0.01s	2.79E−10		4.82E−11	
1/16	1/16	0.07s	6.10E−11	2.19	2.99E−12	4.01
1/32	1/32	0.42s	1.47E−11	2.05	1.87E−13	4.00
1/64	1/64	6.28s	3.65E−12	2.01	1.58E−14	3.56
1/128	1/128	110s	9.09E−13	2.00	1.24E−15	3.68

is fourth-order accurate both in time and space variables if the Richardson extrapolation (5.1) is applied. Additionally, the computational time in seconds is also provided in Table 1-Table 5, as we can see that the computational time for $\Delta t = h = h_x = h_y = \frac{1}{256}$ is less than 10 seconds, and the computational time for $\Delta t = h_x = \frac{1}{256}, h_y = \frac{1}{512}$ is less than 20 seconds. And the method is extremely accurate, the error between the extrapolated solution and exact solution is in the order of 10^{-14} when $\Delta t = h = h_x = h_y = \frac{1}{256}$ and $\Delta t = h_x = \frac{1}{256}, h_y = \frac{1}{512}$, which is nearly the machine accuracy.

To show the unconditional stability of the method, we fix $h = h_x = h_y$ and vary Δt, results using the operator splitting scheme without Richardson extrapolation for $\alpha = 1.2$ and $\alpha = 1.8$ are plotted in Fig. 1. As one can see that these results clearly show that the time step is not related to the spatial meshsize, and as the temporal meshsize goes to zero, the dominant error comes from the spatial part. Moreover, from Fig. 1 we can find that the temporal accuracy of the method is second-order.

Example 2. In this example, we consider the 3D space fractional Allen-Cahn equation with the exact solution

$$u(x, y, t) = e^{-t}x^4(1-x)^4y^4(1-y)^4z^4(1-z)^4. \tag{6.2}$$

The source term and initial condition are given according to this exact solution, in addition, ε is set to be 0.1.

Again, we carry out numerical accuracy test for $1 < \alpha \le 2$. Table 6-Table 9 list the errors and the corresponding convergence orders for $\alpha = 1.2, 1.5, 1.8, 2$ in the L^∞-norm using the same spatial meshsize $h = h_x = h_y = h_z$ while Table 10 lists the errors and the corresponding convergence orders for $\alpha = 1.5$ in the L^∞-norm using different spatial meshsizes. As we can see that these results confirm second-order accuracy in time variable and fourth-order accuracy in space variable if the Richardson extrapolation (5.1) is not applied. But the results is fourth-order accurate both in time and space variables if the Richardson extrapolation (5.1) is applied. Additionally, the computational time in seconds is also provided in Table 6-Table 10, as we can see that the computational time for $\Delta t = h = h_x = h_y = h_z = \frac{1}{128}$ is less than 120 seconds and the computational time for $\Delta t = h_x = \frac{1}{128}, h_y = \frac{1}{160}, h_z = \frac{1}{256}$ is less than 300 seconds. And the method is extremely accurate, the error between the extrapolated solution and exact solution is in the order of 10^{-15} when $\Delta t = h = h_x = h_y = h_z = \frac{1}{128}$ and in the order of 10^{-16} when $\Delta t = h_x = \frac{1}{128}, h_y = \frac{1}{160}, h_z = \frac{1}{256}$, which are both nearly the machine accuracy.

Again, we fix $h = h_x = h_y = h_z$ and vary Δt, numerical results obtained by the operator splitting scheme without Richardson extrapolation for $\alpha = 1.2$ and $\alpha = 1.8$ are plotted in Fig. 2. As one can see that these results clearly show that the time step is not related to the spatial meshsize, and as the temporal meshsize goes to zero, the dominant error comes from the spatial part. Moreover, Fig. 2 shows the temporal second-order accuracy of the method.

Table 7
L^∞-norm errors and CPU times (in seconds) for Example 2 with $\alpha = 1.5$.

Δt	h	CPU	$\|e_1\|_\infty$	order$_1$	$\|e_2\|_\infty$	order$_2$
1/8	1/8	0.01s	2.53E−10		9.13E−11	
1/16	1/16	0.07s	4.61E−11	2.46	5.61E−12	4.02
1/32	1/32	0.42s	1.05E−11	2.14	3.50E−13	4.00
1/64	1/64	6.27s	2.56E−12	2.04	2.19E−14	4.00
1/128	1/128	110s	6.35E−13	2.01	1.37E−15	4.00

Table 8
L^∞-norm errors and CPU times (in seconds) for Example 2 with $\alpha = 1.8$.

Δt	h	CPU	$\|e_1\|_\infty$	order$_1$	$\|e_2\|_\infty$	order$_2$
1/8	1/8	0.01s	2.31E−10		1.51E−10	
1/16	1/16	0.07s	2.90E−11	2.99	9.19E−12	4.04
1/32	1/32	0.42s	5.53E−12	2.39	5.71E−13	4.01
1/64	1/64	6.26s	1.28E−12	2.12	3.57E−14	4.00
1/128	1/128	110s	3.12E−13	2.03	2.23E−15	4.00

Table 9
L^∞-norm errors and CPU times (in seconds) for Example 2 with $\alpha = 2.0$.

Δt	h	CPU	$\|e_1\|_\infty$	order$_1$	$\|e_2\|_\infty$	order$_2$
1/8	1/8	0.01s	2.22E−10		1.91E−10	
1/16	1/16	0.06s	1.92E−11	3.53	1.15E−11	4.05
1/32	1/32	0.42s	2.93E−12	2.71	7.13E−13	4.01
1/64	1/64	6.23s	7.17E−13	2.03	4.44E−14	4.00
1/128	1/128	109s	1.79E−13	2.00	2.78E−15	4.00

Table 10
L^∞-norm errors and CPU times (in seconds) for Example 2 with $\alpha = 1.5$ using unequal meshsizes in x, y and z directions.

Δt	h_x	h_y	h_z	CPU	$\|e_1\|_\infty$	order$_1$	$\|e_2\|_\infty$	order$_2$
1/8	1/8	1/10	1/16	0.02s	2.06E−10		5.94E−11	
1/16	1/16	1/20	1/32	0.10s	4.33E−11	2.25	3.53E−12	4.07
1/32	1/32	1/40	1/64	0.96s	1.03E−11	2.07	2.11E−13	4.06
1/64	1/64	1/80	1/128	17.2s	2.54E−12	2.02	1.30E−14	4.03
1/128	1/128	1/160	1/256	280.s	6.34E−13	2.00	8.29E−16	3.97

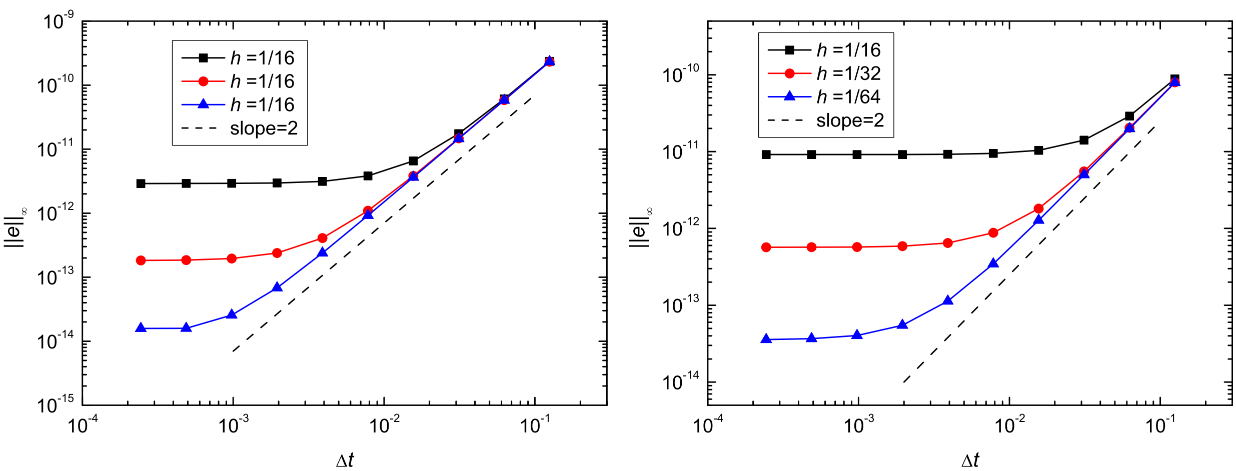

(a) $\alpha = 1.2$ (b) $\alpha = 1.8$

Fig. 2. Numerical results for Example 2 with fixed h but varying Δt.

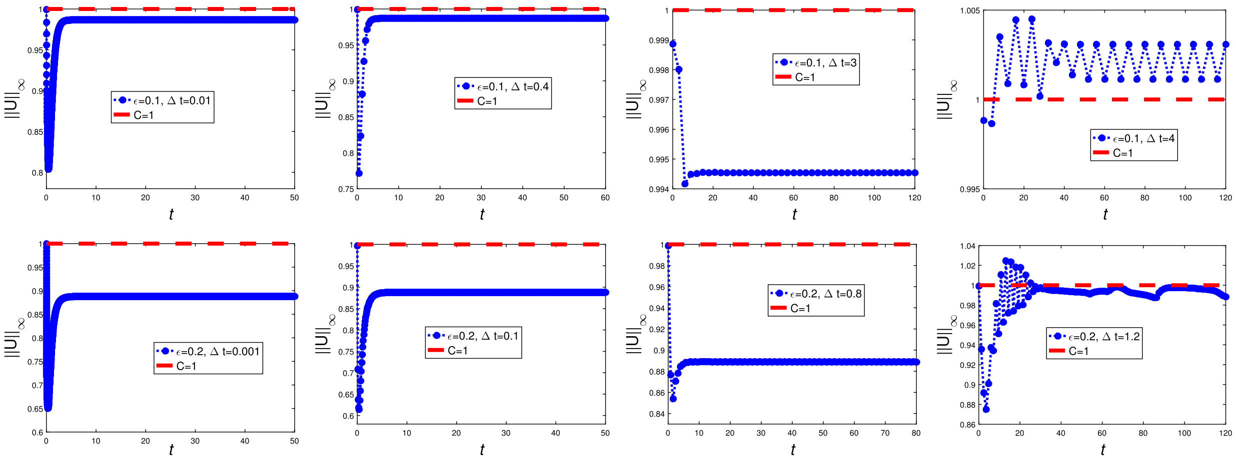

Fig. 3. Maximum values of solutions for Example 3 with fixed α and h but with different Δt and ε, where $\alpha = 1.6$ and $h = 0.05$.

6.2. Numerical tests for discrete maximum principle

In this subsection, we will numerically test the discrete maximum principle by using the numerical scheme (2.4), (2.29)-(2.31) and (2.6) with non-smooth initial conditions.

Example 3. In this example, we consider the 2D space fractional Allen-Cahn equation with initial condition

$$u_0(x, y) = 0.95 \times \mathrm{rand}(x, y) + 0.05, \tag{6.3}$$

where zero boundary values are set for the initial condition $u_0(x, y)$. Moreover, α is set to be 1.7.

For this example, we fix $h = h_x = h_y = 0.05$ but vary ε and Δt. For $\varepsilon = 0.1$, the maximum principle condition (4.4) requires $0.1508 \le \Delta t \le 0.4358$. The top four sub-figures in Fig. 3 show that the maximum values of the numerical solutions are bounded by 1 if $\Delta t = 0.01$, $\Delta t = 0.4$, and $\Delta t = 3$ but exceed 1 if $\Delta t = 4$. For $\varepsilon = 0.2$, the maximum principle condition (4.4) requires $0.0377 \le \Delta t \le 0.1089$. The lower four sub-figures in Fig. 3 show the maximum values of the numerical solutions are bounded by 1 if $\Delta t = 0.001$, $\Delta t = 0.1$, and $\Delta t = 0.8$ but exceed 1 if $\Delta t = 1.2$. These numerical results suggest that the constraint (4.4) for time step size to achieve the discrete maximum principle is only a sufficient condition. In practice, the maximum principle is still valid if a time step size with much smaller values or larger values is adopted.

Example 4. In this example, we consider the 2D space fractional Allen-Cahn equation with initial condition

$$u_0(x, y) = 0.1 \times \mathrm{rand}(x, y) - 0.05, \tag{6.4}$$

where zero boundary values are set for the initial condition $u_0(x, y)$.

In this example, we first fix $h = h_x = h_y = 0.01, \alpha = 1.7$ and $\varepsilon = 0.02$ but vary Δt. The maximum principle condition (4.4) requires $0.1776 \le \Delta t \le 0.4945$. Fig. 4 shows the maximum values of the numerical solutions are bounded by 1 when $\Delta t = 0.01$ and $\Delta t = 0.4$. However, the maximum value exceeds 1 when Δt increases to 2.

Physically, negative values of u in the fractional Allen-Cahn equation represent one phase of material and positive values of u represent another phase of material. Now we investigate the effects of fractional diffusion on phase separation and coarsening process. We set $h = h_x = h_y = 0.01, \varepsilon = 0.02, \Delta t = 0.5$ and $\alpha = 1.2, 1.5, 1.8$. Starting from random initial values, the snapshots of the contours for the numerical solutions at $t = 5, 20, 40, 80$ are shown in Fig. 5. We see that reducing the fractional order yields to a thinner interfaces that allows smaller bulk regions and a much more heterogeneous phase structure. Moreover, it becomes slower for the phase coarsen process when the fractional order becomes smaller.

We also investigate the discrete energy evolution with respect to time. According to (1.4), the discrete energy is calculated by

$$E^n = h_x h_y \sum_{j=1}^{N_x} \sum_{k=1}^{N_y} \left(\frac{1}{4} \left((u_{j,k}^n)^2 - 1 \right)^2 - \frac{\varepsilon^2}{2} u_{j,k}^n \left([\Delta_x^\alpha u^n]_{j,k} + [\Delta_y^\alpha u^n]_{j,k} \right) \right)$$

and the discrete energy changing rate is calculated by

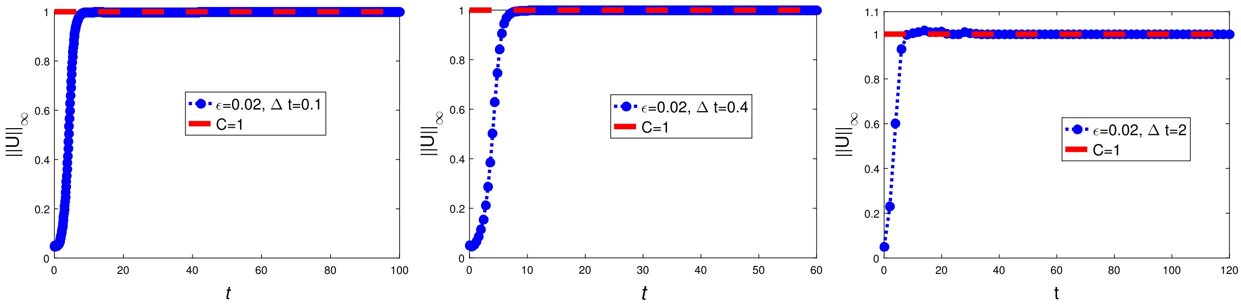

Fig. 4. Numerical results for Example 4 with $\alpha = 1.7, \varepsilon = 0.02, h = 0.01$: the maximum values of solution with different Δt.

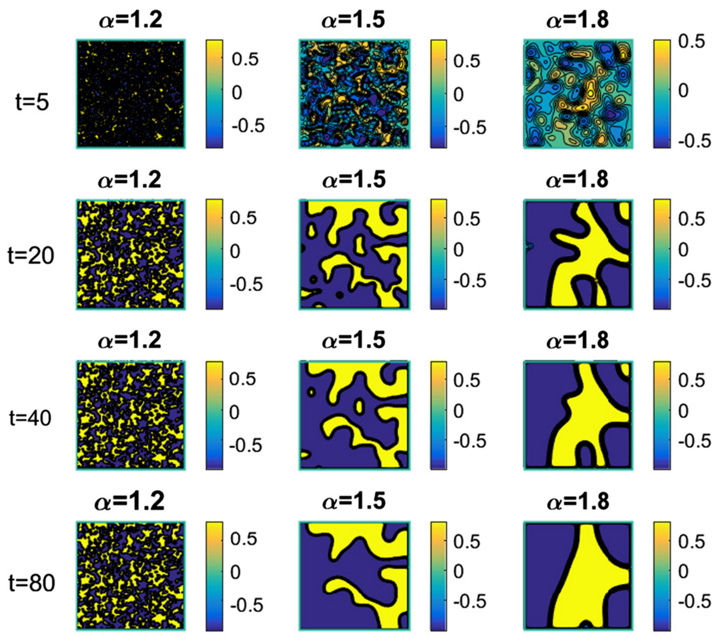

Fig. 5. Numerical dynamics (contour plots) for Example 4 with different fractional derivatives: $\alpha = 1.2, 1.5, 1.8$, where $h = 0.01, \varepsilon = 0.02, \Delta t = 0.5$. (For interpretation of the colors in the figure(s), the reader is referred to the web version of this article.)

$$\frac{E^{n+1} - E^n}{\Delta t}.$$

The evolution of discrete energy and energy changing rate are given in Fig. 6, where $\alpha = 1.7, \varepsilon = 0.02, h = h_x = h_y = 0.01, \Delta t = 0.1, T = 3$. It can be seen that the energy does not always decrease and the energy changing rate is not always negative, which implies that the energy dissipation property are generally not true for the proposed scheme.

Example 5. In this example, we consider the 3D space fractional Allen-Cahn equation with exact solution

$$u_0(x, y, z) = 0.1 \times rand(x, y, z) - 0.05, \tag{6.5}$$

where zero boundary values are set for the initial condition $u_0(x, y, z)$.

Again in this example, we first fix $h = h_x = h_y = h_z = 0.01, \alpha = 1.7, \varepsilon = 0.02$ but vary Δt. The maximum principle condition (4.4) also gives $0.1776 \le \Delta t \le 0.4945$ since the condition (4.4) does not rely on the dimension of the problem. Same as the 2D case, Fig. 7 shows the maximum values of the numerical solutions are bounded by 1 when $\Delta t = 0.1$ and $\Delta t = 0.4$. However, discrete maximum principle is invalid when Δt increases to 2.

Finally, we also investigate the effects of fractional diffusion on phase separation and coarsening process. We set $h = h_x = h_y = h_z = 0.01, \varepsilon = 0.02, \Delta t = 0.5$ and $\alpha = 1.2, 1.5, 1.8$. Starting from random initial values, the snapshots of the contours for the numerical solutions at $t = 5, 20, 40, 80$ on the plane $z = 0.5$ are shown in Fig. 8. Again, we see that reducing the fractional order yields to a thinner interfaces and it becomes slower for the phase coarsen process when the fractional order becomes smaller.

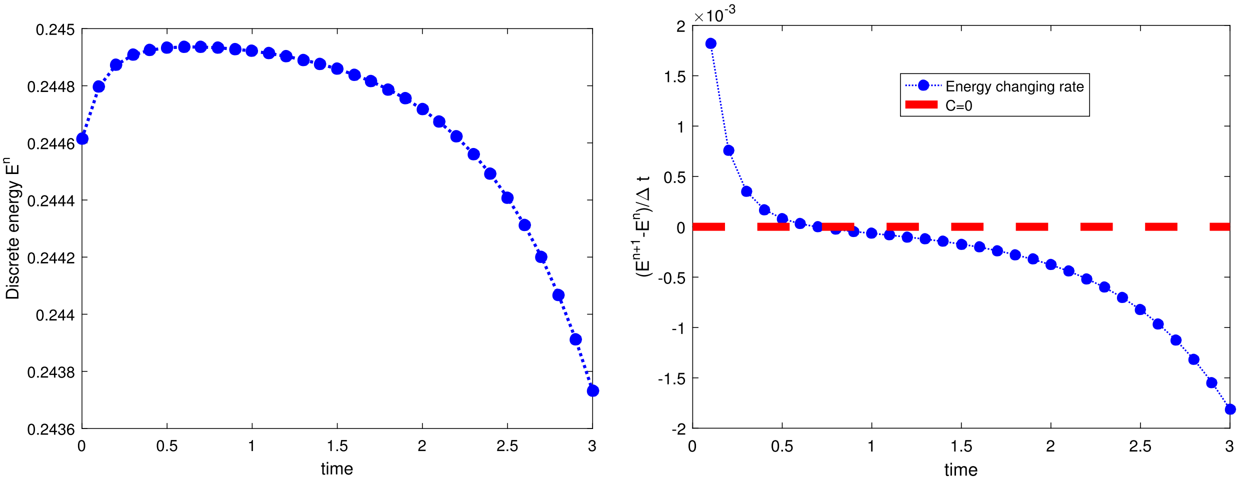

Fig. 6. The evolution of discrete energy and energy changing rate for Example 4 with $\alpha = 1.7$, $\varepsilon = 0.02$, $h = 0.01$.

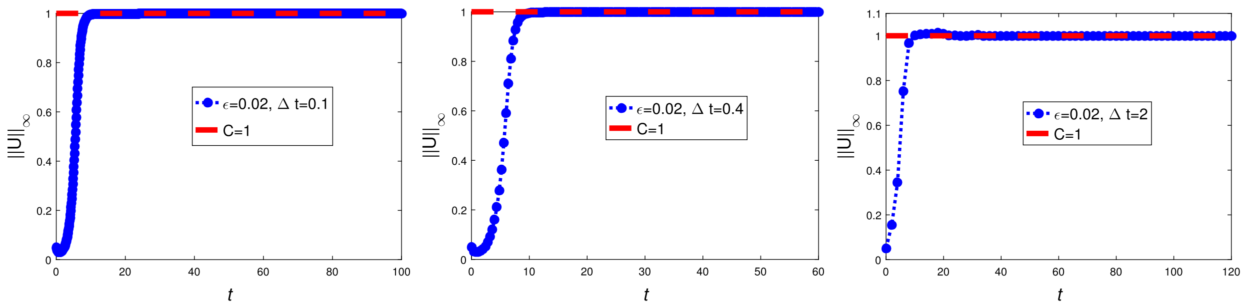

Fig. 7. Numerical results for Example 5 with $\alpha = 1.7$, $\varepsilon = 0.02$ and $h = 0.01$: the maximum values of solution with different Δt.

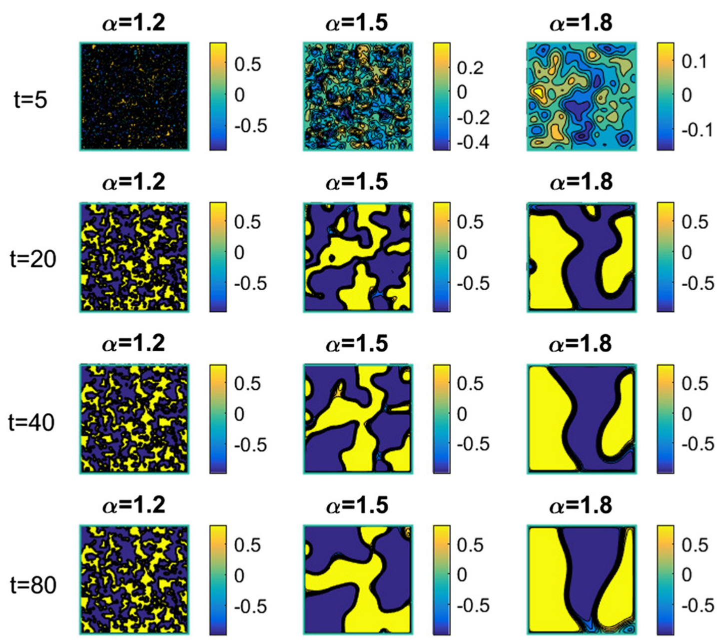

Fig. 8. Numerical dynamics (contour plots on the plane $z = 0.5$) for Example 5 with different fractional derivatives: $\alpha = 1.2, 1.5, 1.8$, where $h = 0.01$, $\varepsilon = 0.02$, $\Delta t = 0.5$.

7. Conclusions

In this paper, we developed a spatial fourth-order maximum principle preserving operator splitting scheme for the space fractional Allen-Cahn equation. The second-order splitting method for the fractional Allen-Cahn equation converts the numerical procedure at each time step into three sub-steps. A simple analysis for first and third sub-steps together with a Fourier analysis for second sub-step show that the proposed operator splitting scheme is unconditionally stable in L^2-norm. Additionally, under certain reasonable time step constraint, the discrete maximum principle in L^∞-norm is also obtained. However, the discrete energy decay property is generally not satisfied for the proposed method. It will be very interesting to develop high-order linearized schemes for the space fractional Allen-Cahn equations with both discrete maximum principle and energy dissipative property.

In addition to the operator splitting scheme, the newly developed extrapolation cascadic multigrid method [31,32] may also be a good choice for quickly solving such high-dimensional fractional differential equations. The research on these aspects will be studied in our future work.

Acknowledgements

Dongdong He was supported by the president's fund-research start-up fund from the Chinese University of Hong Kong, Shenzhen (PF01000857). Kejia Pan was supported by Science Challenge Project (TZ2016002), the National Natural Science Foundation of China (41874086), the Excellent Youth Foundation of Hunan Province of China (2018JJ1042) and the Innovation-Driven Project of Central South University (2018CX042). Hongling Hu was supported by the Construct Program of the Key Discipline in Hunan Province and the Research Foundation of Education Bureau of Hunan Province, China (18B002).

References

[1] S.M. Allen, J.W. Cahn, A microscopic theory for antiphase boundary motion and its application to antiphase domain coarsening, Acta Metall. 27 (1979) 1085–1095.
[2] A. Bueno-Orovio, D. Kay, K. Burrage, Fourier spectral methods for fractional-in-space reaction-diffusion equations, BIT Numer. Math. 54 (2014) 937–954.
[3] K. Burrage, N. Hale, D. Kay, An efficient implicit FEM scheme for fractional-in-space reaction-diffusion equations, SIAM J. Sci. Comput. 34 (2012) A2145–A2172.
[4] C. Çelik, M. Duman, Crank-Nicolson method for the fractional diffusion equation with the Riesz fractional derivative, J. Comput. Phys. 231 (2012) 1743–1750.
[5] H. Chan, J. Wei, Traveling wave solutions for bistable fractional Allen-Cahn equations with a pyramidal front, J. Differ. Equ. 262 (2017) 4567–4609.
[6] B. Chen, D. He, K. Pan, A linearized high-order combined compact difference scheme for multi-dimensional coupled Burgers' equations, Numer. Math., Theory Methods Appl. 11 (2018) 299–320.
[7] J.W. Choi, H.G. Lee, et al., An unconditionally gradient stable numerical method for solving the Allen-Cahn equation, Physica A 388 (2009) 1791–1803.
[8] M. Dehghan, M. Abbaszadeh, W. Deng, Fourth-order numerical method for the space-time tempered fractional diffusion-wave equation, Appl. Math. Lett. 73 (2017) 120–127.
[9] Q. Du, C. Liu, X. Wang, A phase field approach in the numerical study of the elastic bending energy for vesicle membranes, J. Comput. Phys. 198 (2004) 450–468.
[10] L.C. Evans, H.M. Sooner, P.E. Souganidis, Phase transitions and generalized motion by mean curvature, Commun. Pure Appl. Math. 45 (1992) 1097–1123.
[11] L.C. Evans, J. Spruck, Motion of level sets by mean curvature, I, J. Differ. Geom. 33 (1991) 635–681.
[12] X. Feng, A. Prohl, Numerical analysis of the Allen-Cahn equation and approximation for mean curvature flows, Numer. Math. 94 (2003) 33–65.
[13] X. Feng, H. Song, et al., Nonlinearly stable implicit-explicit methods for the Allen-Cahn equation, Inverse Probl. Imaging 7 (2013) 679–695.
[14] C. Gui, M. Zhao, Traveling wave solutions of Allen-Cahn equation with a fractional Laplacian, Ann. Inst. Henri Poincaré, Anal. 32 (2015) 785–812.
[15] Z. Hao, Z. Sun, A linearized high-order difference scheme for the fractional Ginzburg-Landau equation, Numer. Methods Partial Differ. Equ. 33 (2017) 105–124.
[16] D. He, K. Pan, An unconditionally stable linearized CCD-ADI method for generalized nonlinear Schrödinger equations with variable coefficients in two and three dimensions, Comput. Math. Appl. 73 (2017) 2360–2374.
[17] D. He, K. Pan, An unconditionally stable linearized difference scheme for the fractional Ginzburg-Landau equation, Numer. Algorithms 79 (2018) 899–925.
[18] D. He, K. Pan, A fifth-order combined compact difference scheme for Stokes flow on polar geometries, East Asian J. Appl. Math. 7 (2018) 714–727.
[19] D. He, K. Pan, Maximum norm error analysis of an unconditionally stable semi-implicit scheme for multi-dimensional Allen-Cahn equations, Numer. Methods Partial Differ. Equ. 35 (2019) 955–975.
[20] T. Hou, T. Tang, J. Yang, Numerical analysis of fully discretized Crank-Nicolson scheme for fractional-in-space Allen-Cahn equations, J. Sci. Comput. 72 (2017) 1214–1231.
[21] M. Ilíc, F. Liu, et al., Numerical approximation of a fractional-in-space diffusion equation, Fract. Calc. Appl. Anal. 8 (2005) 323–341.
[22] T.A.M. Langlands, B.I. Henry, The accuracy and stability of an implicit solution method for the fractional diffusion equation, J. Comput. Phys. 205 (2005) 719–736.
[23] H.G. Lee, J.Y. Lee, A semi-analytical Fourier spectral method for the Allen-Cahn equation, Comput. Math. Appl. 68 (2014) 174–184.
[24] H.G. Lee, J.Y. Lee, A second order operator splitting method for Allen-Cahn type equations with nonlinear source terms, Physica A 432 (2015) 24–34.
[25] X.J. Li, C.J. Xu, A space-time spectral method for the time fractional diffusion equation, SIAM J. Numer. Anal. 47 (2009) 2108–2131.
[26] X. Lin, K. Michael, H. Sun, A multigrid method for linear systems arising from time-dependent two-dimensional space-fractional diffusion equations, J. Comput. Phys. 336 (2017) 69–86.
[27] Y.M. Lin, C.J. Xu, Finite difference/spectral approximations for the time-fractional diffusion equation, J. Comput. Phys. 225 (2007) 1533–1552.
[28] C. Liu, J. Shen, A phase field model for the mixture of two incompressible fluids and its approximation by a Fourier-spectral method, Physica D 179 (2003) 211–228.
[29] H. Moghaderi, M. Dehghan, et al., Spectral analysis and multigrid preconditioners for two-dimensional space-fractional diffusion equations, J. Comput. Phys. 350 (2017) 992–1011.
[30] Y. Nec, A.A. Nepomnyashchy, A.A. Golovin, Front-type solutions of fractional Allen-Cahn equation, Physica D 237 (2008) 3237–3251.

[31] K. Pan, D. He, et al., A new extrapolation cascadic multigrid method for three dimensional elliptic boundary value problems, J. Comput. Phys. 344 (2017) 499–515.
[32] K. Pan, D. He, H. Hu, An extrapolation cascadic multigrid method combined with a fourth-order compact scheme for 3D Poisson equation, J. Sci. Comput. 70 (2017) 1180–1203.
[33] K. Pan, X. Jin, D. He, Pointwise error estimates of a linearized difference scheme for strongly coupled fractional Ginzburg-Landau equations, Math. Methods Appl. Sci. (2019), https://doi.org/10.1002/mma.5897.
[34] J. Pan, R. Ke, et al., Preconditioning techniques for diagonal-times-Toeplitz matrices in fractional diffusion equations, SIAM J. Sci. Comput. 36 (2014) A2698–A2719.
[35] H. Pang, H. Sun, Multigrid method for fractional diffusion equations, J. Comput. Phys. 231 (2012) 693–703.
[36] D. Peaceman, H. Rachford, The numerical solution of parabolic and elliptic differential equations, J. Soc. Ind. Appl. Math. 3 (1955) 28–41.
[37] A. Saadatmandi, M. Dehghan, A tau approach for solution of the space fractional diffusion equation, Comput. Math. Appl. 62 (2011) 1135–1142.
[38] J. Shen, T. Tang, J. Yang, On the maximum principle preserving schemes for the generalized Allen-Cahn equation, Commun. Math. Sci. 14 (2016) 1517–1534.
[39] J. Shen, X. Yang, Numerical approximations of Allen-Cahn and Cahn-Hilliard equations, Discrete Contin. Dyn. Syst. 28 (2010) 1669–1691.
[40] F. Song, C. Xu, G. Karniadakis, A fractional phase-field model for two-phase flows with tunable sharpness: algorithms and simulations, Comput. Methods Appl. Mech. Eng. 305 (2016) 376–404.
[41] G. Strang, On the construction and comparison of difference schemes, SIAM J. Numer. Anal. 5 (1968) 506–517.
[42] H. Sun, L. Li, A CCD-ADI method for unsteady convection-diffusion equations, Comput. Phys. Commun. 185 (2014) 790–797.
[43] T. Tang, J. Yang, Implicit-explicit scheme for the Allen-Cahn equation preserve the maximum principle, J. Comput. Math. 34 (2016) 451–461.
[44] W. Tian, W.H. Zhou, W. Deng, A class of second order difference approximation for solving space fractional diffusion equations, Math. Comput. 84 (2015) 1703–1727.
[45] P. Wang, C. Huang, Split-step alternating direction implicit difference scheme for the fractional Schrödinger equation in two dimensions, Comput. Math. Appl. 71 (2016) 1114–1128.
[46] P. Wang, C. Huang, An implicit midpoint difference scheme for the fractional Ginzburg-Landau equation, J. Comput. Phys. 312 (2016) 31–49.
[47] N. Wang, C. Huang, An efficient split-step quasi-compact finite difference method for the nonlinear fractional Ginzburg-Landau equations, Comput. Math. Appl. 75 (2018) 2223–2242.
[48] P. Wang, C. Huang, L. Zhao, Point-wise error estimate of a conservative difference scheme for the fractional Schrödinger equation, J. Comput. Appl. Math. 306 (2016) 231–247.
[49] X. Yang, Error analysis of stabilized semi-implicit method of Allen-Cahn equation, Discrete Contin. Dyn. Syst., Ser. B 11 (2009) 1057–1070.
[50] J. Yang, Q. Du, W. Zhang, Uniform L^p-bound of the Allen-Cahn equation and its numerical discretization, Int. J. Numer. Anal. Model. 15 (2018) 213–227.
[51] X. Yang, J. Feng, et al., Numerical simulations of jet pinching-off and drop formation using an energetic variational phase-field method, J. Comput. Phys. 218 (2006) 417–428.
[52] Q. Yang, F. Liu, I. Turner, Numerical methods for fractional partial differential equations with Riesz space fractional derivatives, Appl. Math. Model. 34 (2010) 200–218.
[53] X. Yang, H. Zhang, et al., The finite volume scheme preserving maximum principle for two-dimensional time-fractional Fokker-Planck equations on distorted meshes, Appl. Math. Lett. 97 (2019) 99–106.
[54] P. Yue, J. Feng, et al., Diffuse-interface simulations of drop coalescence and retraction in viscoelastic fluids, J. Non-Newton. Fluid Mech. 129 (2005) 163–176.
[55] X. Yue, S. Shu, et al., Parallel-in-time multigrid for space-time finite element approximations of two-dimensional space-fractional diffusion equations, Comput. Math. Appl. 78 (2019) 3471–3484.
[56] P. Yue, C. Zhou, et al., Phase-field simulations of interfacial dynamics in viscoelastic fluids using finite elements with adaptive meshing, J. Comput. Phys. 219 (2006) 47–67.
[57] S.B. Yuste, L. Acedo, An explicit finite difference method and a new Von Neumann-type stability analysis for fractional diffusion equations, SIAM J. Numer. Anal. 42 (2005) 1862–1874.
[58] S. Zhai, X. Feng, Y. He, Numerical simulation of the three dimensional Allen-Cahn equation by the high-order compact ADI method, Comput. Phys. Commun. 185 (2014) 449–2455.
[59] S. Zhai, Z. Weng, X. Feng, Fast explicit operator splitting method and time-step adaptivity for fractional non-local Allen-Cahn model, Appl. Math. Model. 40 (2016) 1315–1324.
[60] J. Zhang, Q. Du, Numerical studies of discrete approximations to the Allen-Cahn equation in the sharp interface limit, SIAM J. Sci. Comput. 31 (2009) 3042–3063.
[61] L. Zhang, H. Sun, H. Pang, Fast numerical solution for fractional diffusion equations by exponential quadrature rule, J. Comput. Phys. 299 (2015) 130–143.
[62] P. Zhuang, F. Liu, et al., Numerical methods for the variable-order fractional advection diffusion equation with a nonlinear source term, SIAM J. Numer. Anal. 47 (2009) 1760–1781.